Title

Pathogenic diversification of the gut commensal Providencia alcalifaciens via acquisition of a second type III secretion system.

Journal

Infection and Immunity, 92(10)

Authors

Klein, Jessica

Predeus, Alexander

Greissl, Aimee

et al.

Publication Date

2024-10-15

DOI

10.1128/iai.00314-24

Peer reviewed

AMERICAN SOCIETY FOR MICROBIOLOGY | Infection and Immunity

Host-Microbial Interactions | EBM Contribution

Pathogenic diversification of the gut commensal *Providencia alcalifaciens* via acquisition of a second type III secretion system

Jessica A. Klein,[1] Alexander V. Predeus,[2] Aimee R. Greissl,[1] Mattie M. Clark-Herrera,[1] Eddy Cruz,[3] Jennifer A. Cundiff,[1] Amanda L. Haeberle,[1] Maya Howell,[1] Aaditi Lele,[1] Donna J. Robinson,[1] Trina L. Westerman,[3,4] Marie Wrande,[1] Sarah J. Wright,[1] Nicole M. Green,[5] Bruce A. Vallance,[6] Michael McClelland,[7] Andres Mejia,[8] Alan G. Goodman,[1,9] Johanna R. Elfenbein,[3,4] Leigh A. Knodler[1,10]

AUTHOR AFFILIATIONS See affiliation list on p. 27.

ABSTRACT *Providencia alcalifaciens* is a Gram-negative bacterium found in various water and land environments and organisms, including insects and mammals. Some *P. alcalifaciens* strains encode gene homologs of virulence factors found in pathogenic Enterobacterales members, such as *Salmonella enterica* serovar Typhimurium and *Shigella flexneri*. Whether these genes are pathogenic determinants in *P. alcalifaciens* is not known. In this study, we investigated *P. alcalifaciens*–host interactions at the cellular level, focusing on the role of two type III secretion systems (T3SS) belonging to the Inv-Mxi/Spa family. $T3SS_{1b}$ is widespread in *Providencia* spp. and encoded on the chromosome. A large plasmid that is present in a subset of *P. alcalifaciens* strains, primarily isolated from diarrheal patients, encodes for $T3SS_{1a}$. We show that *P. alcalifaciens* 205/92 is internalized into eukaryotic cells, lyses its internalization vacuole, and proliferates in the cytosol. This triggers caspase-4-dependent inflammasome responses in gut epithelial cells. The requirement for the $T3SS_{1a}$ in entry, vacuole lysis, and cytosolic proliferation is host cell type-specific, playing a more prominent role in intestinal epithelial cells than in macrophages or insect cells. In a bovine ligated intestinal loop model, *P. alcalifaciens* colonizes the intestinal mucosa and induces mild epithelial damage with negligible fluid accumulation in a $T3SS_{1a}$- and $T3SS_{1b}$-independent manner. However, $T3SS_{1b}$ was required for the rapid killing of *Drosophila melanogaster*. We propose that the acquisition of two T3SS has allowed *P. alcalifaciens* to diversify its host range, from a highly virulent pathogen of insects to an opportunistic gastrointestinal pathogen of animals.

KEYWORDS type III secretion, virulence, pathogenesis, enteric bacteria, diarrhea

Despite belonging to a large and clinically significant family of Gram-negative bacteria, *Providencia* species remain among the least studied members of Enterobacteriaceae. *Providencia* spp. colonize diverse hosts and environments. In addition to being found in soil (1), water (2), sewage (3), and retail meats, fruits, and vegetables (4–7), *Providencia* spp. are members of the human gut, oral cavity, and sputum microbiomes (8–12). *Providencia* spp. have also been isolated from numerous animals, including penguins, turtles, sharks, snakes (13), nematodes (14), and insects such as blow flies, fruit flies, house flies, and olive flies (13, 15–18). Notably, some *Providencia* spp. are pathogenic to *Drosophila melanogaster, Ceratitis capitata* (Mediterranean fruit fly), and *Anastrepha ludens* (Mexican fruit fly), with the most highly virulent species being *Providencia alcalifaciens* and *Providencia sneebia* in *D. melanogaster* (13) and *P. alcalifaciens* and *Providencia rustigianii* in *A. ludens* (19).

Considered opportunistic bacterial pathogens of humans, *P. alcalifaciens*, *Providencia rettgeri*, and *Providencia stuartii* are the most common clinical isolates (20, 21) and cause a spectrum of nosocomial and environmentally acquired diseases, including urinary

Editor Andreas J. Bäumler, University of California Davis, Davis, California, USA

Address correspondence to Leigh A. Knodler, leigh.knodler@med.uvm.edu.

Mattie M. Clark-Herrera, Eddy Cruz, Jennifer A. Cundiff, Amanda L. Haeberle, Maya Howell, Aaditi Lele, Donna J. Robinson, Trina L. Westerman, Marie Wrande, and Sarah J. Wright contributed equally to this article. Author order was determined alphabetically by surname.

The authors declare no conflict of interest.

Received 22 July 2024
Accepted 13 August 2024
Published 10 September 2024

tract, wound and ocular infections, diarrhea, meningitis, and sepsis. *Providencia* spp. are typically resistant to penicillins, first-generation cephalosporins, aminoglycosides, tetracyclines, and polymyxins (22, 23). Increasing antimicrobial resistance is a major public health concern (24, 25). Several groups have reported *P. alcalifaciens* to be a cause of diarrhea in infants and travelers in developing countries (21, 26–30) and in foodborne-associated outbreaks (31–33). The incidence of *P. alcalifaciens* in diarrheal patients in Thailand (1.9%), Bangladesh (2.1%) and Kenya (3.2%) is on par with *Salmonella* spp. (4, 29, 34). A higher incidence of *P. alcalifaciens* (10%–18%) has been reported for persons with traveler's diarrhea (21, 35). *P. alcalifaciens* has also been associated with diarrhea in dogs and cats (36–39). Previous work has verified the ability of some *P. alcalifaciens* clinical isolates to elicit diarrheal disease in a removable intestinal tie adult rabbit diarrhea (RITARD) infection model (40, 41) and cause fluid accumulation in rabbit ileal loops (31) and diarrhea in suckling mice (42). Furthermore, clinical strains isolated from patients with diarrhea exhibit varying invasive abilities, with some *P. alcalifaciens* being highly invasive for human epithelial cell lines e.g., HeLa, HEp-2, Vero and Caco-2, and others being noninvasive (31, 43–49). Despite a strong association with diarrheal illness in humans and animals, a detailed understanding of the pathogenic mechanisms of *P. alcalifaciens* is lacking.

Enteric pathogens such as *Salmonella enterica* serovar Typhimurium (*S*. Typhimurium) and *Shigella flexneri* use type III secretion systems (T3SSs), also known as injectisomes, to deliver "effector" proteins that modulate the actin cytoskeleton, allowing for efficient bacterial entry into non-phagocytic cells. T3SSs are found in many (but not all) *Providencia* isolates, including *P. alcalifaciens* (50), an indication of the pathogenic potential of members of this genus. We reported earlier that *P. alcalifaciens* 205/92, a clinical isolate, encodes for two T3SSs belonging to the Inv-Mxi/Spa family, which we designated $T3SS_{1a}$ and $T3SS_{1b}$ (51). *Sodalis glossinidius* (52), an insect endosymbiont, and some isolates of *Providencia* spp. are the only other bacteria known to encode for two Inv-Mxi/Spa T3SS. *P. alcalifaciens* $T3SS_{1a}$ is closely related to, and functionally interchangeable with, the invasion-associated T3SS1 from *S*. Typhimurium (51). Structural proteins of $T3SS_{1b}$ share significant amino acid sequence identity to those of the Ysa T3SS from *Yersinia enterocolitica* (51), which is restricted to biotype 1B (53). Neither Ysa nor $T3SS_{1b}$ translocator operons functionally substitute for those of *S*. Typhimurium in driving bacterial entry into non-phagocytic cells, suggesting an evolutionary functional divergence within the Inv-Mxi/Spa family of T3SSs (51).

We hypothesized that T3SSs are virulence determinants in *P. alcalifaciens*. In this study, we have investigated the role of the two T3SSs in bacterial colonization of mammalian and insect cells, specifically human intestinal epithelial cells (IECs), human macrophages, and *D. melanogaster* macrophage-like cells. We report that *P. alcalifaciens* 205/92 enters eukaryotic cells, rapidly lyses its internalization vacuole, and then replicates within the cytosol. We further show that $T3SS_{1a}$ is encoded on a 128-kb plasmid and is necessary for efficient bacterial entry, nascent vacuole lysis, and intracellular replication in human IECs. In human macrophages, a $T3SS_{1a}$ mutant induces less host cell cytotoxicity than wild-type bacteria. While a $T3SS_{1b}$ mutant exhibits no colonization defect in mammalian or insect cell lines, it is significantly attenuated for the infection of *D. melanogaster*. Therefore, *P. alcalifaciens* 205/92 uses two type III injectisomes to colonize diverse eukaryotic hosts.

RESULTS

P. alcalifaciens 205/92 genome

Seven *P. alcalifaciens* genomes have been sequenced as part of the NIH Common Fund Human Microbiome Project (54) and deposited in GenBank, including *P. alcalifaciens* 205/92 (https://www.ncbi.nlm.nih.gov/datasets/genome/GCF_000527335.1/). This strain was initially isolated from a young Bangladeshi boy having diarrhea (43, 46). The contig-level genome assembly includes 88 contigs. We generated a complete *P. alcalifaciens* 205/92 genome using a combination of Oxford Nanopore Technologies

(ONT) long-read and Illumina short-read sequencing. Assembly of the highest-quality 100 x filtered and trimmed Nanopore reads (see *Methods* section) using Trycycler generated three circular replicons: a 4,094,134-bp chromosome and two plasmids, 127,796 bp (p128kb) and 40,541 bp (p41kb) in size. Due to size selection, smaller plasmids are often under-represented in long-read-only assemblies. To account for this, we performed an independent hybrid assembly of the Nanopore reads with bbduk-trimmed Illumina reads, which allowed us to recover a third plasmid, 3,997 bp in size (p4kb). Polishing the resulting combined assembly with Polypolish using the bbduk-trimmed Illumina reads corrected three errors in the chromosome and two in the 128-kb plasmid. The GenBank accession number is GCA_038449115.1.

The *P. alcalifaciens* 205/92 complete genome has a G + C content of 41.8%, in line with the average G + C content of *Providencia* spp. genomes (55). Automated annotation of the assembled genome using Bakta identified 4,007 protein-coding genes (3,842, 113, 46, and six proteins coded on the chromosome, p128kb, p41kb, and p4kb plasmids, respectively), as well as seven ribosomal operons (22 rRNA genes overall), and 80 tRNA genes. Using the PHASTER prophage-prediction web tool followed by manual curation, we identified nine putative prophage regions (Fig. 1A). Genomic islands encoding flagella, a type VI secretion system (T6SS) and a type III secretion system, $T3SS_{1b}$, were present on the chromosome (Fig. 1A). Genomic islands associated with a type IV secretion system (T4SS) and a second type III secretion system, $T3SS_{1a}$ (Fig. 1B), were found on p41kb and p128kb, respectively.

We compared the *P. alcalifaciens* 205/92 genome with other available *P. alcalifaciens* genomes (Fig. 1). Core genome alignment identified 44,562 high-quality (AGCT-only) variant positions alongside 3,937,741 constant sites. Phylogenetic analysis of the resulting whole-genome alignment using IQTree (www.iqtree.org/doc/Substitution-Models) identified an TVM + F + I + R2 model as best fitting the data according to the Bayesian information criterion. *P. rustigianii* strain 52579_F01 was used as an outgroup. Phylogenetic analysis of the strains (Fig. 1C) generally confirmed the conclusions made previously based on protein-coding-based phylogeny (50): strains designated as *P. alcalifaciens* could be divided into two highly distinct clusters (Fig. 1C and D). Cluster 1, which includes strain 205/92 and a closely related strain 2939/90 also isolated in Bangladesh from a child with diarrhea (40), has much closer and fewer differences between the sequenced genomes and far more isolated strains than cluster 2, which could be the result of a fast and recent spread of Cluster 1. We checked for the presence of $T3SS_{1a}$ and $T3SS_{1b}$ in different *P. alcalifaciens* strains that were chosen according to the phylogeny from the two major clusters. The chromosomal-encoded $T3SS_{1b}$ was fully present in all the profiled strains (Fig. 1A). For the plasmid-encoded $T3SS_{1a}$, our analysis was limited to those strains with the largest plasmid (Fig. 1B and C). Cluster 1 is characterized by a much higher presence of the two large plasmids identified in the 205/92 strain. Indeed, out of 34 isolates that belong to cluster 1, four carried a full (defined as read coverage is >80%), and 13 carried a partial representation of the 128-kb plasmid (read coverage is 40%–80%). Notably, there was a strong correlation between isolates from diarrheal patients, either humans or dogs (indicated by red asterisks in Fig. 1C), and the presence of p128kb (Fig. 1C). These isolates were sourced from diverse geographical locations (Table S1). In contrast, only three out of 11 isolates from cluster 2 carried a partial p128kb. We were surprised to find that, despite the considerable differences in the overall genetic content of this plasmid between strains, the coding potential for all $T3SS_{1a}$ structural and regulatory proteins remained intact in all the strains (Fig. 1B; Fig. S1). Interestingly, there was considerable heterogeneity between strains in the protein-coding sequence length for a predicted type III effector, SipA. In *P. alcalifaciens* 205/92, SipA is a > 2,300 AA protein (Fig. 1B). Nine out of 34 isolates from cluster 1 and none from cluster 2 carried the 41-kb plasmid. The small p4kb plasmid had a more uniform distribution: 5/34 for cluster 1 and 3/11 for cluster 2 (Fig. 1C). A mean distance between isolates from cluster 1 and cluster 2 was determined to be between 16,000 and 17,000 SNPs per 44,562 high-quality variable positions. Cluster 1 had a mean

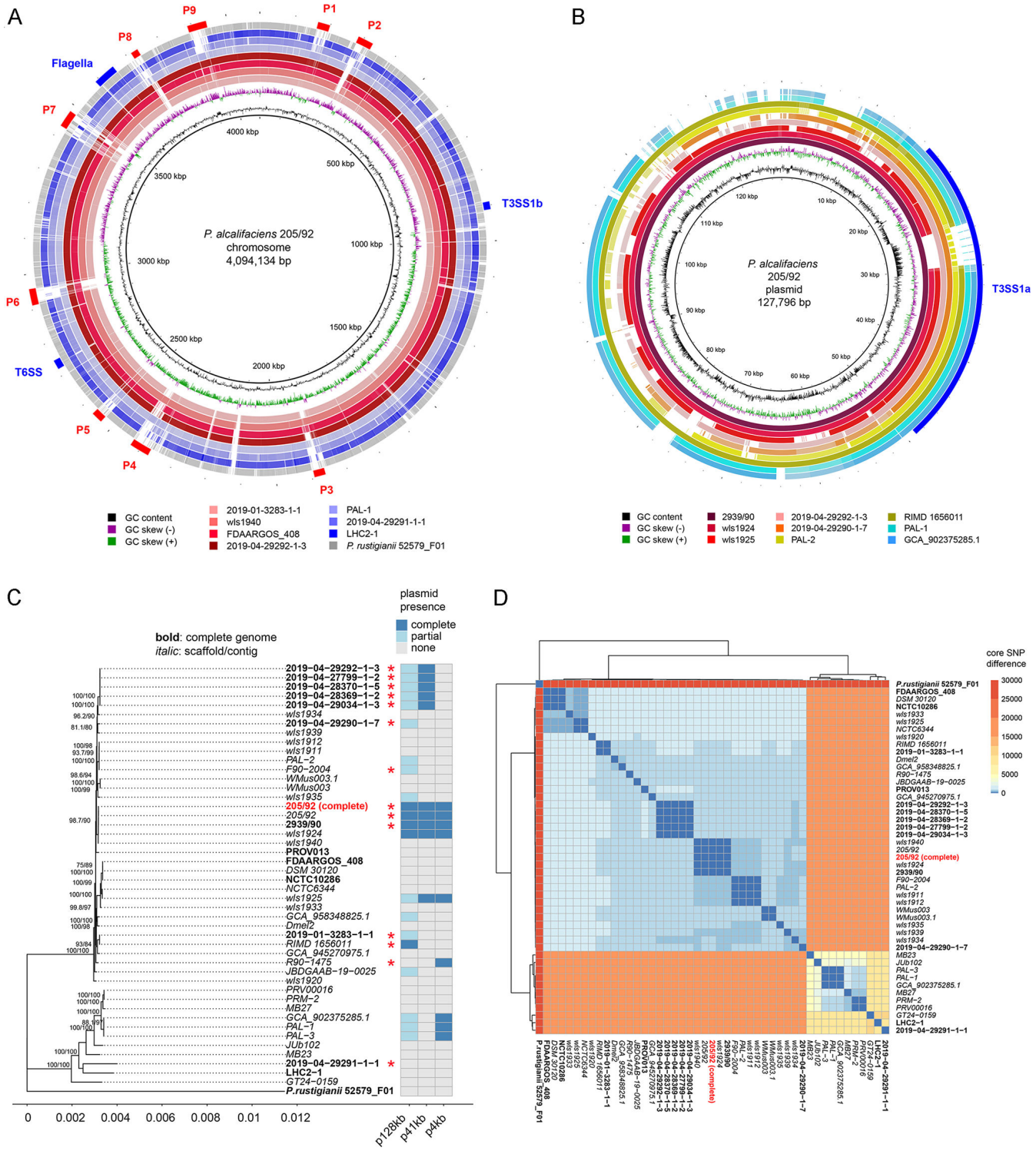

FIG 1 *Providencia alcalifaciens* 205/92 genome. (A) BRIG diagram of chromosome alignment of seven *P. alcalifaciens strains* (2019–01-3283-1-1, wls1940, FDAARGOS_408, 2019–04-29292-1-3, PAL-1, 2019–04-29291-1-1, and LHC2-1) and *P. rustigianii* strain 52579_F01. The complete genome of strain 205/92 presented in this work is used as a reference. Shades of red indicate the phylogenetic branch that includes 205/92; shades of blue indicate the second major branch. Exact coordinates of putative prophages P1–P9, flagella, and secretion systems are provided in Table S1. (B) BRIG diagram of p128kb alignment from nine *P. alcalifaciens* strains (2939/90, wls1924, wls1925, 2019–04-29292-1-3, 2019–04-29290-1-7, PAL-2, RIMD 1656011, PAL-1, and GCA_902375285.1). p128kb of the 205/92 strain presented in this work is used as a reference. Shades of blue indicate strains from the second phylogenetic branch that does not include 205/92. Exact coordinates of $T3SS_{1a}$ are provided in Table S1. (C) Whole-genome phylogenetic tree generated with IQTree from the core genome alignment of

(Continued on next page)

Fig 1 (Continued)

46 *P. alcalifaciens* strains and *P. rustigianii* strain 52579_F01 used as an outgroup. The bold font indicates complete genome assemblies; the italic font indicates genomes assembled into multiple contigs or scaffolds. The heatmap indicates the presence (complete or partial) or absence of the three plasmids present in the *P. alcalifaciens* 205/92 genome. The plasmid is classified as complete if the read coverage is >80%; as partial if the read coverage is 40%–80%; and absent if read coverage is <40%. Red asterisks denote isolates collected from human or canine patients with diarrhea (see Table S1 for detailed information on strains). Note that source information is available for all strains. (D) A heatmap of pairwise core SNP distances between the 45 *P. alcalifaciens* strains and *P. rustigianii* strain 52579_F01. The total number of identified high-quality (AGCT-only) variable positions is 44,562.

distance between the two strains of approximately 1,000 SNPs; at the same time, the mean distance between the two strains in cluster 2 was over 5,000 SNPs (Fig. 1D). Overall, we conclude that the *P. alcalifaciens* species is genomically diverse and consists of two major lineages (50).

T3SS$_{1a}$ genes are induced in the late-log phase of growth

Given the involvement of secretion systems in the pathogenesis of numerous Gram-negative bacteria, we initially set out to define *in vitro* growth conditions under which *P. alcalifaciens* T3SS genes are transcriptionally active. The upstream regulatory regions of *invF, prgH, and sicA*, the first genes in predicted operons from T3SS$_{1a}$ and T3SS$_{1b}$ pathogenicity islands (Fig. 2A), were cloned upstream of a promoterless *luxCDABE* in pFU35. The resulting plasmids were electroporated into wild-type (WT) *P. alcalifaciens*. We detected robust luminescence for bacteria carrying P*prgH*$_{1a}$-*luxCDABE* and P*invF*$_{1a}$-*luxCDABE* transcriptional reporters at the late log-phase of growth in LB–Miller broth, pH 7.0, at 37°C (Fig. 2B and C). Transcriptional activity for *sicA*$_{1a}$ was much lower, but still greater than that of the promoter-less vector, pFU35, under these conditions (Fig. 2C). By contrast, no luminescence was detected for bacteria carrying T3SS$_{1b}$ gene reporters under any of the *in vitro* growth conditions we tested, i.e., shaking in LB–Miller broth, pH 7.0 (Fig. 2C) or pH 5.8 at 37°C or 25°C; shaking in M9 minimal media pH 7.0 at 37°C or 25°C; or McCoy's medium or Schneider's medium in the absence or presence of 10% heat-inactivated calf serum at 25°C and 37°C (data not shown). Collectively, we conclude that T3SS$_{1a}$- and T3SS$_{1b}$-associated genes are expressed under distinct conditions.

Salmonella spp. secrete effector proteins into culture media in a type III secretion-dependent manner (56). When *P. alcalifaciens* was grown under *in vitro* conditions that induce T3SS$_{1a}$-associated genes (late-log phase in LB–Miller broth), numerous proteins were secreted into the culture supernatant (Fig. 2D). To identify whether protein secretion was dependent on T3SS$_{1a}$ or T3SS$_{1b,}$ we compared the protein profiles of culture supernatants from WT, Δ*invA*$_{1a,}$ and Δ*invA*$_{1b}$ bacteria. InvA is a highly conserved inner membrane component of the Inv-Mxi/Spa T3SS family. A *S.* Typhimurium *invA* mutant is unable to assemble the needle portion of the injectisome and, as a result, is deficient for T3SS-dependent protein secretion (57). By analogy, we presume that *P. alcalifaciens invA* deletion mutants are type III secretion-incompetent. The secreted protein profile of Δ*invA*$_{1b}$ bacteria was indistinguishable from that of WT bacteria. In contrast, two major protein bands, one at >250 kDa and one at ~40 kDa, and numerous minor protein bands were absent from the supernatants of Δ*invA*$_{1a}$ bacteria (Fig. 2D). Mass spectrometric analysis identified the most abundant proteins as SipA$_{1a}$ (predicted molecular mass of 240 kDa) and a mixture of SipC$_{1a}$ and SipD$_{1a}$ (predicted mass of 43 and 39 kDa, respectively), the corresponding genes of which are encoded on T3SS$_{1a}$ (Fig. 2A). In *Salmonella* spp., SipA is a type III effector with actin-binding properties (58), SipC is a type III translocator protein (59), and SipD is the needle tip protein of T3SS1 (59). Due to the presence of tandem repeat sequences, *P. alcalifaciens* 205/92 SipA$_{1a}$ is much larger than orthologous proteins from *S.* Typhimurium (SipA), *Shigella flexneri* (IpaA) (~74 kDa), and some other *P. alcalifaciens* strains. Of the 20 *P. alcalifaciens* strains harboring p128kb, 11 encode for SipA$_{1a}$ of >200 kDa (Fig. 1B; Fig. S1).

Providencia spp. have peritrichous flagella and are considered motile. *P. alcalifaciens* 205/92 encodes numerous flagella-associated genes in one large genetic island on

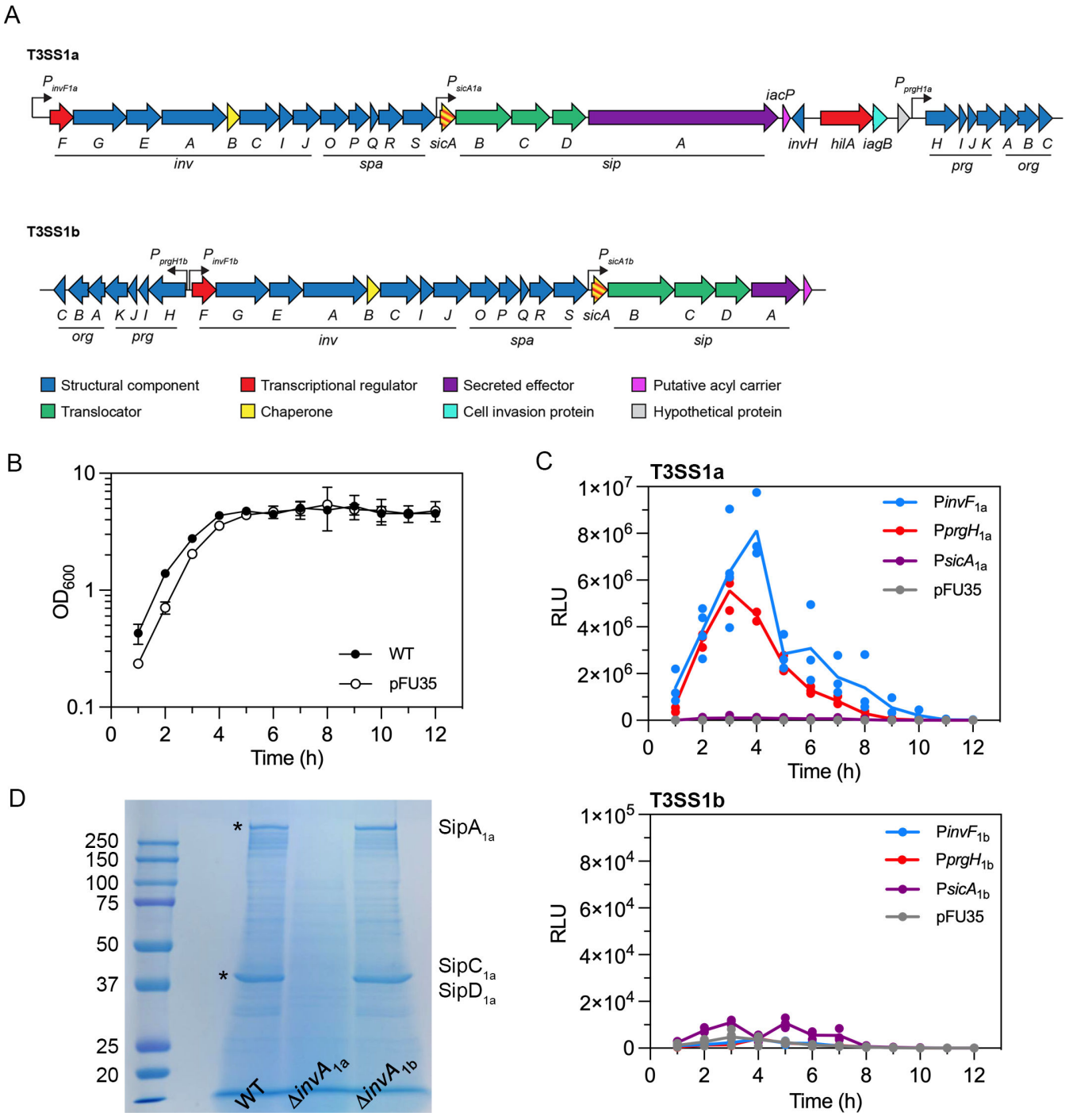

FIG 2 Characterization of $T3SS_{1a}$ and $T3SS_{1b}$ in *P. alcalifaciens* 205/92. (A) Cartoon depiction of the genetic organization of $T3SS_{1a}$ and $T3SS_{1b}$. (B) Growth curve of *P. alcalifaciens* 205/92 WT and WT carrying pFU35 plasmid. Bacterial subcultures were grown at 37°C, with shaking at 220 rpm in LB–Miller broth, and OD_{600} measured hourly. Mean ± SD of three independent experiments. (C) Bacterial luminescence over a time course of growth. *P. alcalifaciens* 205/92 carrying *luxCDABE* transcriptional reporters for the indicated $T3SS_{1a}$ (upper panel) or $T3SS_{1b}$ (lower panel) gene promoters or the empty plasmid (pFU35) were grown as in (B), and relative light units (RLU) were measured every hour by using a microplate reader. Lines indicate the mean of three independent experiments (each symbol represents data from one experiment). (D) Secreted protein profile. *P. alcalifaciens* WT, Δ$invA_{1a}$, and Δ$invA_{1b}$ subcultures were grown for 4 hours in LB–Miller broth. Supernatants were collected, filtered, and precipitated proteins separated by SDS-PAGE and stained with GelCode Blue. Molecular mass markers are shown on the left. The protein bands indicated by asterisks were excised and identified as $SipA_{1a}$ (>250 kDa), $SipC_{1a}$ (~40 kDa), and $SipD_{1a}$ (~40 kDa) by mass spectrometry.

the chromosome (Fig. 1A; Fig. S2A). We constructed *luxCDABE*-based transcriptional reporters to the upstream regulatory regions of *flhD*, *flgB,* and *fliC* and measured bacterial luminescence when WT bacteria carrying these reporters were grown in LB–Miller broth pH 7.0 at 37°C for 12 hours. All three genes were transcribed, with a peak of transcription at the late log-phase of growth (Fig. S2B). Swimming motility of *P. alcalifaciens* was evident on soft agar plates, albeit much less than that of *S*. Typhimurium WT bacteria but greater than that of a non-motile *S*. Typhimurium Δ*flgB* mutant (Fig. S2C). Overall, we conclude that *P. alcalifaciens* $T3SS_{1a}$ and flagellar genes are induced by aeration and at the late log-phase of growth, similar to T3SS1 and flagellar genes in *S*. Typhimurium (60).

Internalization of *P. alcalifaciens* into mammalian and insect cell lines

Some clinical isolates of *P. alcalifaciens*, including 205/92, have been reported to invade HEp-2 cell monolayers (43, 46). To investigate the phenotypic characteristics of the initial interaction of *P. alcalifaciens* 205/92 with non-phagocytic mammalian cells, we used scanning electron microscopy (SEM) and transmission electron microscopy (TEM). *P. alcalifaciens* were grown under conditions that induce the $T3SS_{1a}$ (Fig. 2C), added to monolayers (HeLa or HCT116 epithelial cells), centrifuged for 5 minutes, and incubated for a further 15 minutes (20 minutes post-infection (p.i.) for SEM) or 55 minutes (1 h p.i. for TEM) at 37°C, and then infected monolayers were processed for microscopy. By SEM, we observed *P. alcalifaciens* attaching to filopodial extensions on the epithelial cell surface (Fig. 3A and C). Sometimes, these membrane protrusions were wrapped around the bacteria (Fig. 3A). Similar initial interactions with epithelial cells have been described for *S. flexneri*, *Y. enterocolitica,* and *Helicobacter pylori* (61–64). Invasion of *P. alcalifaciens* into epithelial cells is associated with actin condensation at the site of bacterial entry (40) and inhibited by cytochalasin D (43), a hallmark of the "trigger" type of cell entry mediated by *S*. Typhimurium and *S. flexneri*. By SEM, we did not observe dramatic plasma membrane ruffles, which are characteristic of bacterial entry via this mechanism, however (Fig. 3C). TEM analysis suggested that *P. alcalifaciens* internalization into non-phagocytic cells was instead via a zipper-like mechanism; upon bacterial adherence, membrane protrusions formed and wrapped around bacteria in tight apposition, eventually engulfing the entire bacterium (Fig. 3B and D).

As *P. alcalifaciens* is known to colonize mammalian and insect hosts, we tested whether its entry into different types of eukaryotic cells was T3SS-dependent. *P. alcalifaciens* 205/92 WT and Δ*invA* deletion mutants were grown under conditions that induce the $T3SS_{1a}$ (Fig. 2C) before their addition to mammalian and insect cells. Internalized bacteria were enumerated at 1 h p.i. using the gentamicin protection assay, and invasion efficiency was calculated as the proportion of the bacterial inoculum that was internalized. Compared to WT bacteria (set to 100%), Δ$invA_{1a}$ bacteria were highly defective for entry into HCT116 human colonic epithelial cells (15 ± 5.7%; Fig. 3E), a phenotype that could be partially restored by plasmid-borne complementation (Fig. 3E). Deletion of $invA_{1a}$ also affected *P. alcalifaciens* entry into *D. melanogaster* S2 cells (31 ± 9.6%; Fig. 3E), which have characteristics of fly hemocytes. In macrophages derived from the human monocytic cell line, THP-1, there was no difference in the internalization efficiency of the three bacterial strains (Fig. 3E) in accordance with the phagocytic properties of these cells. By contrast, the invasion efficiency of Δ$invA_{1b}$ bacteria was equivalent to that of WT bacteria in HCT116, THP-1, and S2 cells (Fig. 3E). Overall, we conclude that *P. alcalifaciens* $T3SS_{1a}$ is required for efficient bacterial internalization into human IECs and insect cells, suggesting a role for the $T3SS_{1a}$-dependent translocation of type III effectors in this entry process.

Intracellular replication of *P. alcalifaciens*

We next investigated whether *P. alcalifaciens* 205/92 can survive and replicate intracellularly in mammalian and insect cells. In HCT116 epithelial cells, there was a 3.3-fold increase in recoverable CFUs for WT bacteria over a 12-h time course (Fig. 4A, left panel), with the greatest net increase in intracellular proliferation occurring between 1 h p.i. and

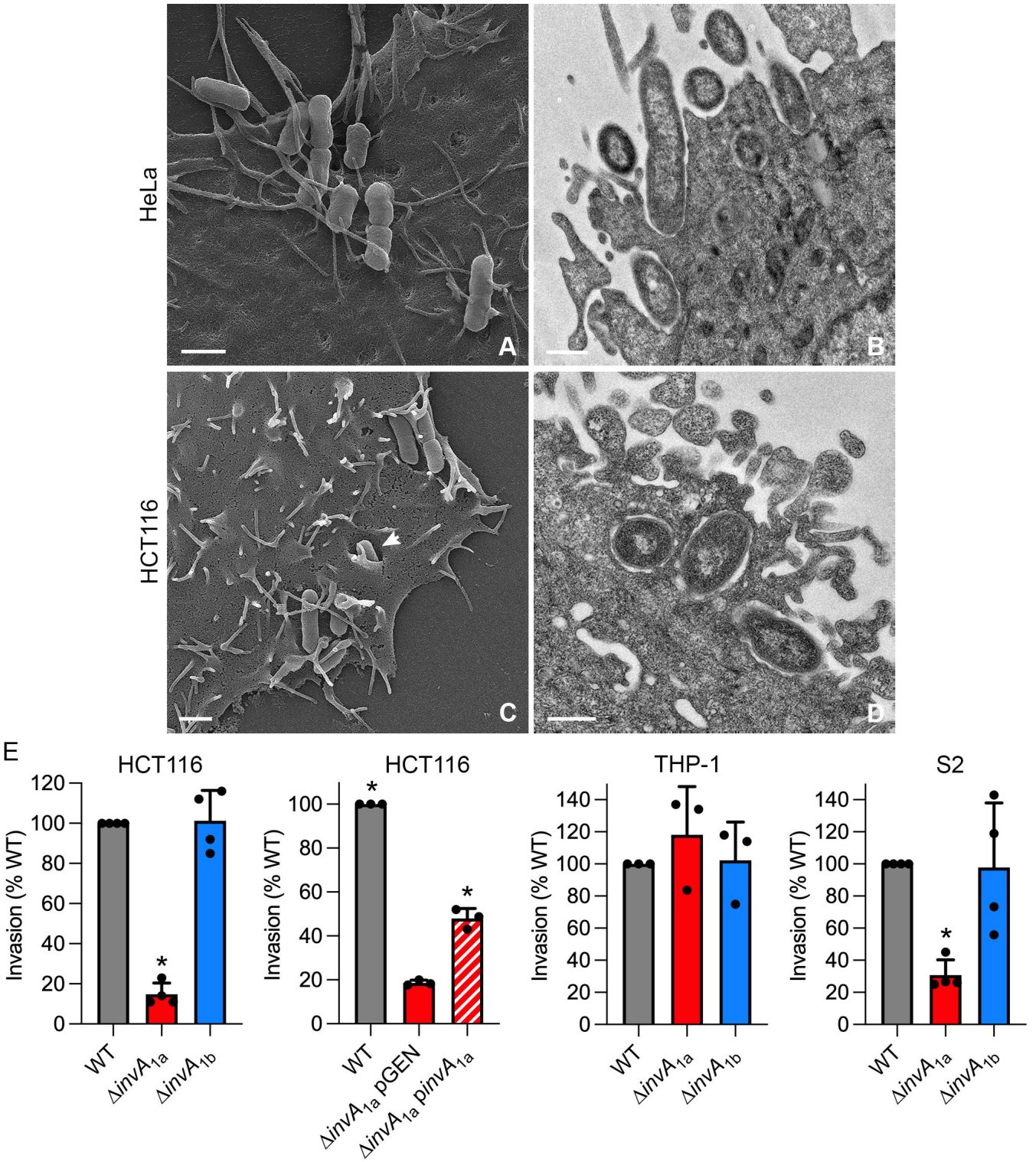

FIG 3 *P. alcalifaciens* adherence to, and invasion of, eukaryotic cells. (A) Scanning electron micrograph (SEM) of *P. alcalfaciens* 205/92 associating with filopodia on the surface of a HeLa epithelial cell at 20 minutes p.i. The scale bar is 1 µm. (B) Transmission electron micrograph (TEM) showing *P. alcalifaciens* entering a HeLa cell at 1 h p.i. The scale bar is 0.5 µm. (C) SEM shows bacteria associating with filopodia on the surface of a HCT116 colonic epithelial cell at 20 minutes p.i. One bacterium is seen entering via a zipper-like mechanism (indicated by arrowhead). The scale bar is 1 µm. (D) TEM showing *P. alcalfaciens* entering a HCT116 cell at 1 h p.i. The scale bar is 0.5 µm. (E) HCT116, THP-1, and S2 cells were infected with bacterial subcultures at MOIs of ~150, ~10, and ~5, respectively. Invasion efficiencies of *P. alcalifaciens* WT, Δ*invA*$_{1a}$, Δ*invA*$_{1a}$ carrying pGEN-MCS (empty vector) or pGEN-*invA*$_{1a}$ (complemented strain), and Δ*invA*$_{1b}$ bacteria were

(Continued on next page)

Fig 3 (Continued)

compared by gentamicin protection assay at 1 h p.i. Invasion efficiency is defined as the percentage of the inoculum that was internalized; the invasion efficiency of WT bacteria was normalized to 100% in each experiment. Mean ± SD from three to four independent experiments. Asterisks indicate data significantly different from WT or Δ*invA*$_{1a}$ pGEN bacteria ($P < 0.05$, ANOVA with Dunnett's *post-hoc* test).

4 h p.i. (Fig. 4A, left panel). We confirmed the intracellular proliferation of WT bacteria within epithelial cells using an inside/outside assay in conjunction with fluorescence microscopy. HCT116 cells were infected with *P. alcalifaciens* carrying a plasmid constitutively expressing *dsRed* (pGEN-DsRed.T3), and anti-*P. alcalifaciens* antibodies were used to probe for extracellular bacteria in non-permeabilized cells. The number of intracellular WT bacteria increased from 1 h p.i. (mean of 1.7 bacteria/cell) to 8 h p.i. (mean of 2.92 bacteria/cell) (Fig. 4A, middle panel). Replication of the Δ*invA*$_{1b}$ mutant was indistinguishable from that of WT bacteria in HCT116 cells (Fig. 4A , left and middle panels). However, a progressive decrease in recoverable CFUs for Δ*invA*$_{1a}$ bacteria was observed in the gentamicin protection assay (Fig. 4A, left panel) and there was no evidence of bacterial proliferation at the single-cell level (mean of 1.6 bacteria/cell and 1.8 bacteria/cell at 1 h p.i. and 8 h p.i., respectively) (Fig. 4A, middle panel). Negligible lactate dehydrogenase (LDH) release, a measure of cytotoxicity, was detected over the infection time course irrespective of the infecting bacterial strain (Fig. 4A, right panel).

The patterns of intracellular proliferation for WT bacteria and the deletion mutants were different in human macrophages as compared to human IECs. Using the gentamicin protection assay, there was a decrease in recoverable CFUs for WT bacteria over a 12-h time course of infection in THP-1 cells (Fig. 4B, left panel). Incongruently, there was a slight increase in the mean number of WT bacteria/cell at the single-cell level, from a mean of 1.8 bacteria/cell at 1 h p.i. to 2.6 bacteria/cell at 8 h p.i., (Fig. 4B, middle panel, Fig. S3). However, high levels of cell death/cytotoxicity during WT infection, up to 35% of the monolayer by 12 h p.i. (Fig. 4B, right panel), likely account for the overall decrease in viable CFUs, as assessed by the gentamicin protection assay. Δ*invA*$_{1b}$ bacteria showed a similar profile to WT bacteria for CFUs, number of bacteria/cell, and cytotoxicity induction kinetics (Fig. 4B). By contrast, there was a net increase in Δ*invA*$_{1a}$ bacteria over time, as measured by CFUs and the number of bacteria per cell (mean of 2.0 and 5.2 bacteria/cell at 1 h p.i. and 8 h p.i., respectively), indicating replication of Δ*invA*$_{1a}$ bacteria in THP-1 cells (Fig. 4B). However, significantly less LDH was released into the culture supernatants, suggesting that the overall increase in viable Δ*invA*$_{1a}$ bacteria was explained, in part, by decreased THP-1 cell lysis/detachment of infected cells compared to WT infection (Fig. 4B).

Notably, the level of bacterial replication was higher in insect cells than in mammalian cells. Upon *P. alcalifaciens* infection of *D. melanogaster* S2 cells, there was an overall increase in intracellular CFUs over 12 hours for WT (6.2-fold), Δ*invA*$_{1a}$ (4.2-fold), and Δ*invA*$_{1b}$ bacteria (5.6-fold) (Fig. 4C). Similarly, the mean number of bacteria per S2 cell increased from 1 h p.i. to 8 h p.i. for all three strains (2.2 to 4.7 bacteria/cell for WT, 1.5 to 3.8 bacteria/cell for Δ*invA*$_{1a}$, and 2.2 to 3.8 bacteria/cell for Δ*invA*$_{1b}$; Fig. 4C, middle panel, Fig. S3). The colorimetric assay for LDH release cannot be used with S2 cells (65), so we could not assess host cell cytotoxicity concurrently with CFUs for *Providencia*-S2 cell infections. Collectively, these data indicate that *P. alcalifaciens* 205/92 can replicate intracellularly in mammalian and insect cells, and the contribution of T3SS$_{1a}$ to bacterial proliferation and induction of host cell death is both host- and cell-type dependent.

Intracellular expression kinetics of T3SS$_{1a}$ and T3SS$_{1b}$

To follow *P. alcalifaciens* gene expression after internalization into mammalian and insect cells, we infected HCT116 and S2 cells with WT bacteria carrying plasmid-borne P*invF*$_{1a}$-*luxCDABE* or P*prgH*$_{1a}$-*luxCDABE* as T3SS$_{1a}$ reporters or P*invF*$_{1b}$-*luxCDABE* or P*prgH*$_{1b}$-*luxCDABE* as T3SS$_{1b}$ reporters. At various time points p.i., infected monolayers were collected, lysed, and luminescence associated with intracellular bacteria quantified

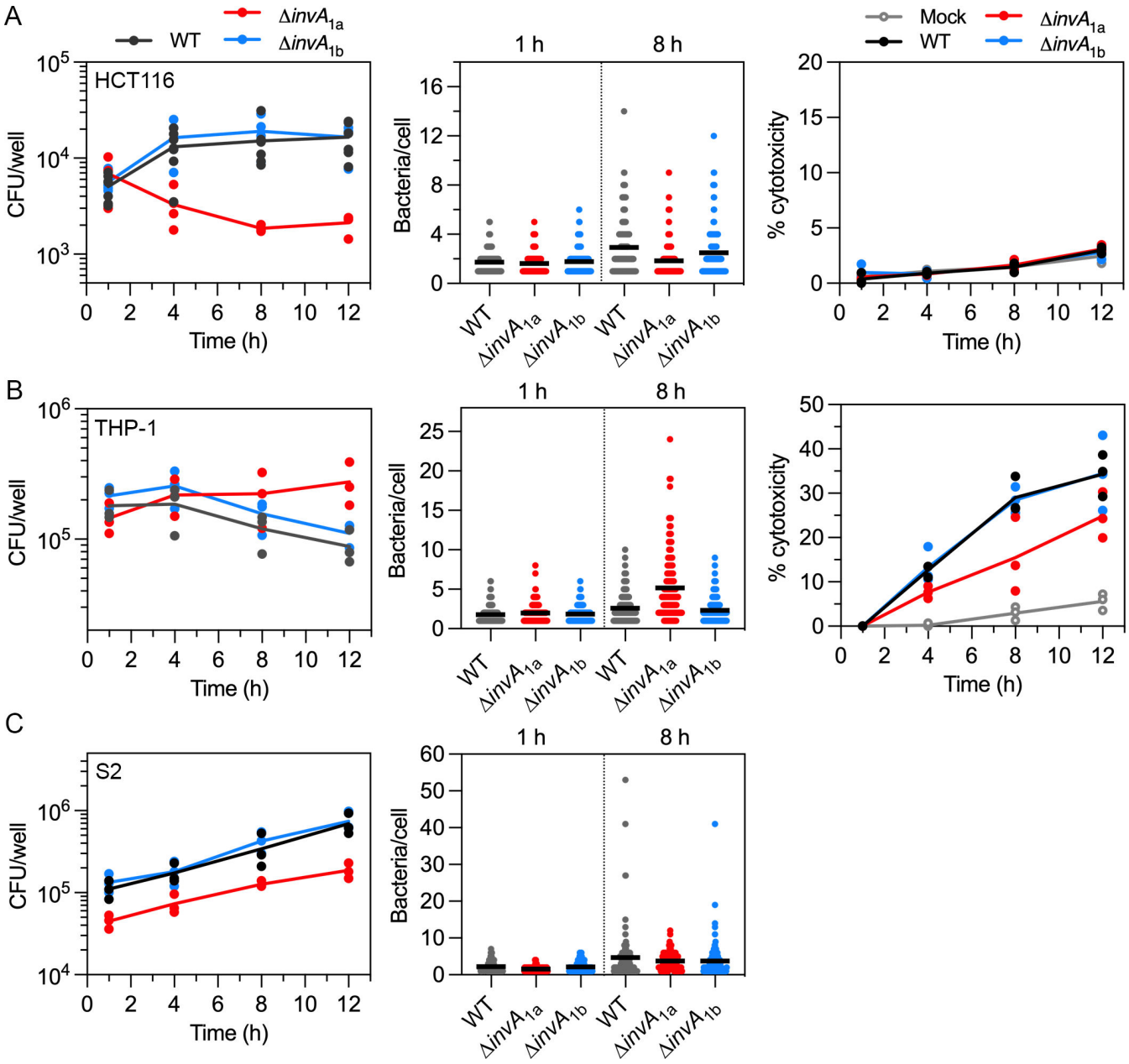

FIG 4 Intracellular replication of *P. alcalifaciens* in eukaryotic cells. (A) Intracellular proliferation of WT, Δ*invA*$_{1a}$, and Δ*invA*$_{1b}$ bacteria in HCT116 cells was quantified by the gentamicin protection assay (left panel, *n* = 3 independent experiments, where each dot represents the mean from one experiment) and fluorescence microscopy (middle panel; each dot represents the number of bacteria in one cell, and the horizontal bar indicates the mean of three independent experiments). Infections conditions for WT and Δ*invA*$_{1b}$ bacteria were as described for Fig. 3E (MOI ~ 150). The MOI for Δ*invA*$_{1a}$ bacteria was increased by two- to threefold (MOI ~ 300–450) to increase bacterial internalization. For microscopy experiments, WT, Δ*invA*$_{1a}$, and Δ*invA*$_{1b}$ bacteria were carrying pGEN-DsRed.T3. Inside/outside staining was used to distinguish intracellular from extracellular DsRed-labeled bacteria. Cell death was measured by LDH release into the supernatants (right panel, *n* = 3 independent experiments, where each dot represents the mean from one experiment). Percent cytotoxicity was calculated by normalizing to maximal cell death (1% (vol/vol) Triton X-100 lysis). (B) Intracellular proliferation of WT, Δ*invA*$_{1a}$, and Δ*invA*$_{1b}$ bacteria in THP-1 macrophages (MOI ~ 10 for all strains) was quantified by the gentamicin protection assay (left panel, *n* = 3 independent experiments) and fluorescence microscopy (middle panel, *n* = 3 independent experiments). Cytotoxicity was measured using LDH release assay (right panel, *n* = 3 independent experiments). (C) Intracellular proliferation of WT, Δ*invA*$_{1a}$, and Δ*invA*$_{1b}$ bacteria in S2 cells (MOI ~ 5 for all strains) was quantified by the gentamicin protection assay (left panel, *n* = 3 independent experiments) and fluorescence microscopy (middle panel, *n* = 2 independent experiments).

in a plate reader. We found that the intracellular expression kinetics of *P. alcalifaciens* genes encoded in T3SS$_{1a}$ are comparable to those in *S.* Typhimurium T3SS1 (60).

Specifically, we observed a rapid downregulation of *prgH*$_{1a}$ and *invF*$_{1a}$ gene transcription, such that by 6 h p.i., bacterial luminescence was equivalent to that of the promoterless *luxCDABE* plasmid backbone, pFU35 (Fig. 5). Transcription of *prgH*$_{1b}$ and *invF*$_{1b}$ was not observed over the time course, indicating that T3SS$_{1b}$-associated genes are not induced intracellularly in mammalian or insect tissue culture cells, at least up to 6 h p.i.

P. alcalifaciens colonizes the cytosol of eukaryotic cells

Our earlier work on the SipC/IpaC family of type III translocators showed that these proteins have differential destabilizing activities on bacteria-containing vacuole membranes (66). For example, replacing SipC in *S.* Typhimurium with its ortholog from either of the professional cytosolic pathogens, *S. flexneri* (IpaC) or *Chromobacterium violaceum* (CipC), enables *Salmonella* to lyse its internalization vacuole more efficiently. We used this gene swapping strategy to predict the intracellular niche of *P. alcalifaciens* 205/92. We have previously shown that *P. alcalifaciens* SipC$_{1a}$ can partially complement for the internalization defect of a *S.* Typhimurium Δ*sipC* mutant (Δ*sipC::sipC*$_{1a}$) into non-phagocytic cells (51). Using the chloroquine (CHQ) resistance assay (67, 68), which determines the proportion of internalized bacteria that are present in the cytosol, we found a significantly increased proportion of *S.* Typhimurium Δ*sipC::sipC*$_{1a}$ bacteria in the cytosol of HCT116 epithelial cells and J774A.1 macrophages compared to *S.* Typhimurium WT (Fig. 6A). Notably, the level of nascent vacuole lysis for Δ*sipC::sipC*$_{1a}$ and Δ*sipC::cipC* bacteria was comparable (Fig. 6A). From these results, we speculated that *P. alcalifaciens* is a cytosolic bacterium, like *C. violaceum* (66).

We applied the CHQ resistance assay to *Providencia*-infected HCT116, THP-1, and S2 cells to determine their intracellular replication niche unequivocally. At 90 min p.i., ~80% of WT bacteria were present in the cytosol in all three cell types (Fig. 6B). Therefore, lysis of the nascent bacteria-containing vacuole is fast and efficient. This level of cytosolic presence was sustained at later times (>70% cytosolic bacteria at 8 h p.i.; Fig. 6B), indicating bacterial replication (Fig. 4) occurs in the cytosol of eukaryotic cells. There was no significant difference in the proportion of cytosolic WT and Δ*invA*$_{1b}$ bacteria in any cell type (Fig. 6B). However, a lower proportion of Δ*invA*$_{1a}$ bacteria were present in the cytosol of HCT116 cells at 90 min p.i. and 8 h p.i. (Fig. 6B), indicating a defect in

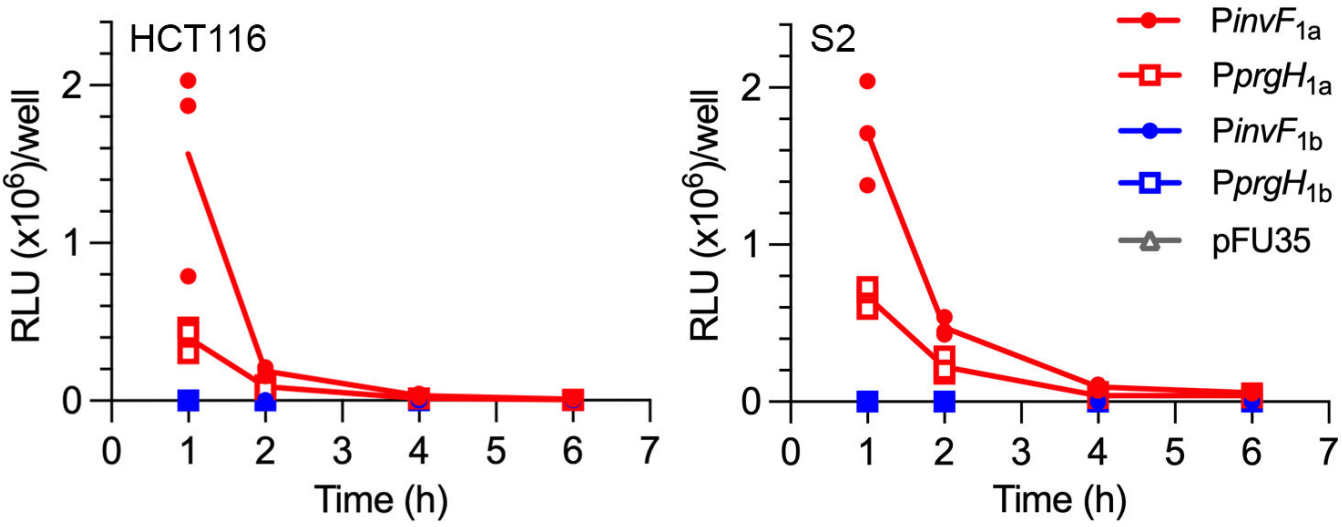

FIG 5 Rapid downregulation of T3SS$_{1a}$ after bacterial internalization. HCT116 (left panel, MOI ~ 150) or S2 (right panel, MOI ~ 5) cells were infected with subcultures of *P. alcalifaciens* WT bacteria carrying one of the following transcriptional reporter plasmids: P*invF*$_{1a}$-*luxCDABE*, P*prgH*$_{1a}$-*luxCDABE*, P*invF*$_{1b}$-*luxCDABE*, P*prgH*$_{1b}$-*luxCDABE*, or the empty vector control (pFU35). At the indicated time points, infected monolayers were collected, lysed, and the luminescence associated with internalized bacteria measured in a plate reader. The line indicates the mean of three independent experiments (each symbol represents data from one experiment).

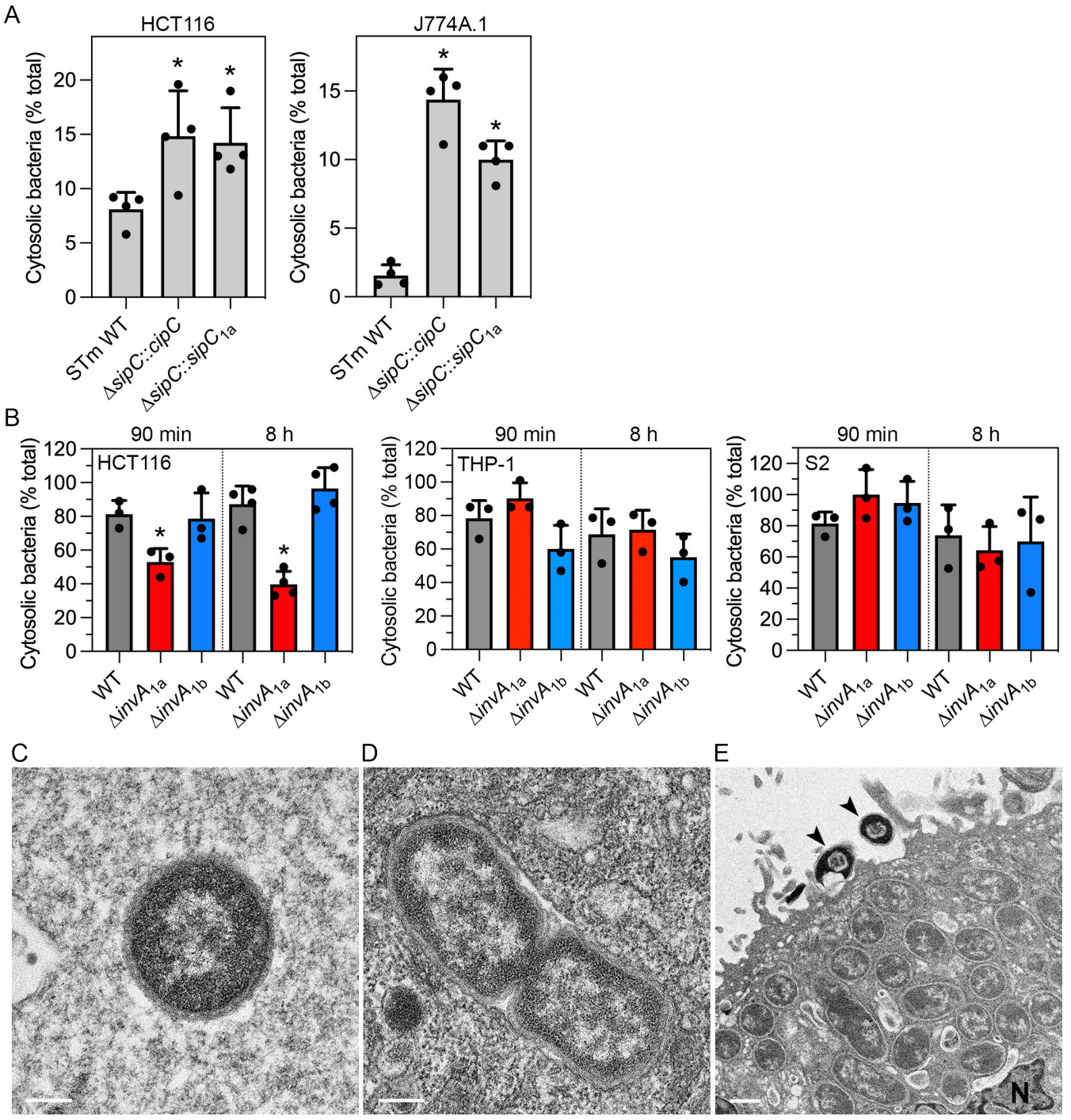

FIG 6 *P. alcalifaciens* lyses its internalization vacuole and then replicates in the cytosol of eukaryotic cells. (A) HCT116 (left panel, MOI ~ 50) or J774A.1 (right panel, MOI ~ 5) cells were infected with *S.* Typhimurium (STm) WT, Δ*sipC::cipC* (chromosomal replacement of *sipC* with *C. violaceum cipC*), or Δ*sipC::sipC*$_{1a}$ (chromosomal replacement of *sipC* with *P. alcalifaciens sipC*$_{1a}$) bacteria, and the proportion of internalized bacteria present in the cytosol at 90 min p.i. was assessed by CHQ resistance assay. Mean ± SD from four independent experiments. Asterisks indicate data significantly different from STm WT bacteria ($P < 0.05$, ANOVA with Dunnett's *post-hoc* test). (B) HCT116 (left panel, MOI ~ 150), THP-1 (middle panel, MOI ~ 10), and S2 (right panel, MOI ~ 5) cells were infected with *P. alcalifaciens* 205/92 WT, Δ*invA*$_{1a}$, and Δ*invA*$_{1b}$ bacteria, and the proportion of cytosolic bacteria at 90 min p.i. and 8 h p.i. was determined by CHQ resistance assay. Mean ± SD from three to four independent experiments. Asterisks indicate data significantly different from WT bacteria ($P < 0.05$, ANOVA with Dunnett's *post-hoc* test). (C and D) Representative TEM images of cytosolic (C) and vacuolar (D) *P. alcalifaciens* in HeLa epithelial cells at 1 h p.i. Scale bars are 200 nm. (E) Representative TEM image of *P. alcalifaciens* replicating in the cytosol of a HeLa epithelial cell at 4 h p.i. The scale bar is 500 nm; *N* = nucleus; arrowheads indicate extracellular bacteria presumably killed by gentamicin.

bacteria-containing vacuole lysis in human IECs. This dependence on $T3SS_{1a}$ for vacuole lysis was not observed in human macrophages or insect cells, however (Fig. 6B).

We used TEM as an independent method to assess the intracellular site of *P. alcalifaciens* in eukaryotic cells. Most WT bacteria were free in the cytosol of epithelial cells by 1 h p.i. (59% cytosolic in HeLa cells, $n = 49$, Fig. 6C; 64% cytosolic in HCT116 cells, $n = 11$). An intact vacuolar membrane was observed around some bacteria in epithelial cells at 1 h p.i. (Fig. 6D). By 4 h p.i., bacterial replication in the cytosol of epithelial cells was evident (Fig. 6E). We also observed bacteria that remain extracellular, seemingly firmly attached to the surface of epithelial cells, which were killed by gentamicin (Fig. 6E). Like epithelial cells, most intracellular WT bacteria were found in the cytosol without any obvious surrounding membrane in THP-1 macrophages (83% cytosolic, $n = 18$) and S2 cells (93% cytosolic, $n = 43$) by 90 min p.i. Collectively, these data support that *P. alcalifaciens* 205/92 rapidly escapes from its internalization vacuole and then replicates in the cytosol of mammalian and insect cells.

Inflammasome activation by *P. alcalifaciens*

Inflammasomes are cytosolic innate immune sensors that play a key role in restricting bacterial infections, and epithelial-intrinsic inflammasomes mediate protective responses against intestinal pathogens such as *S.* Typhimurium (69–71) and *C. rodentium* (72). Considering *P. alcalifaciens* can invade mammalian cells (Fig. 3 and 4) and replicate in the cytosol (Fig. 6), we speculated it would activate human IEC canonical (caspase-1) and/or non-canonical (caspase-4) inflammasomes. We have previously shown that the activation status of murine IECs affects the contribution of non-canonical and canonical inflammasomes to host defense (73). We therefore considered that inflammasome activation in human IECs might also be similarly affected. In agreement with previous reports in HT-29 colonic epithelial cells (74–76), *CASP1* mRNA was significantly upregulated by IFNγ treatment in IECs, specifically HCT116 (Fig. 7A) and Caco-2 C2BBe1 (Fig. S4A) cells. A robust increase in pro-caspase-1 and moderate increase in pro-caspase 4 levels were detected upon IFNγ treatment in HCT116 cells (Fig. 7B). Only pro-caspase-1 was responsive to IFNγ treatment in C2Bbe1 cells (Fig. S4B). Therefore, with IFNγ priming in conjunction with *CASP1*$^{-/-}$ and *CASP4*$^{-/-}$ knockout (KO) cells, we can investigate whether *P. alcalifaciens* 205/92 activates canonical and non-canonical inflammasomes in IECs.

Processing and secretion of two cytokines, interleukin (IL)−18 and IL-1β, is dependent on inflammasome activation. Despite encoding *IL1B* mRNA (77) (Fig. 7A), IL-1β is not secreted by human IECs upon bacterial infection ((78); our unpublished results). We therefore used IL-18 secretion as a readout of inflammasome activation. IL-8 release was a control for an inflammasome-independent cytokine. Upon *Providencia* infection of WT HCT116 cells, IL-18 was detected in the cell culture supernatant at 16 h p.i. in both untreated and IFNγ-primed cells (Fig. 7C). The infection-dependent potentiation of IL-18 release from both untreated and IFNγ-primed cells was statistically significant (Fig. 7C). The magnitude of increase in IL-18 release after *P. alcalifaciens* infection of *CASP1*$^{-/-}$ KO cells was comparable to that of WT HCT116 cells, with and without IFNγ treatment (Fig. 7C). By contrast, IL-18 release was abrogated from infected *CASP4*$^{-/-}$ KO cells, irrespective of IFNγ priming (Fig. 7C). Infection-induced IL-8 secretion was comparable regardless of the priming status or cell genotype (Fig. 7C). These data indicate that *P. alcalifaciens* 205/92 stimulates IL-18 secretion from human IECs in a caspase-4-dependent manner, i.e., via activation of the non-canonical inflammasome.

Previous studies in human IECs have shown that caspase-4 is critical for limiting *S.* Typhimurium replication (69, 78, 79). To test whether IEC intrinsic inflammasomes (caspase-1 and/or caspase-4) influence intracellular proliferation of *P. alcalifaciens* 205/92, we compared bacterial replication. In unprimed HCT116 cells, there was no significant difference in *P. alcalifaciens* replication in WT, *CASP1*$^{-/-}$ or *CASP4*$^{-/-}$ cells over 10 hours (9.2-, 7.6-, and 11.9-fold, respectively; Fig. 7D). IFNγ priming efficiently restricted bacterial replication in WT and *CASP1*$^{-/-}$ HCT116 cells (3.3- and 3.3-fold, respectively) but not *CASP4*$^{-/-}$ cells. Rather, robust bacterial replication was still observed in *CASP4*$^{-/-}$

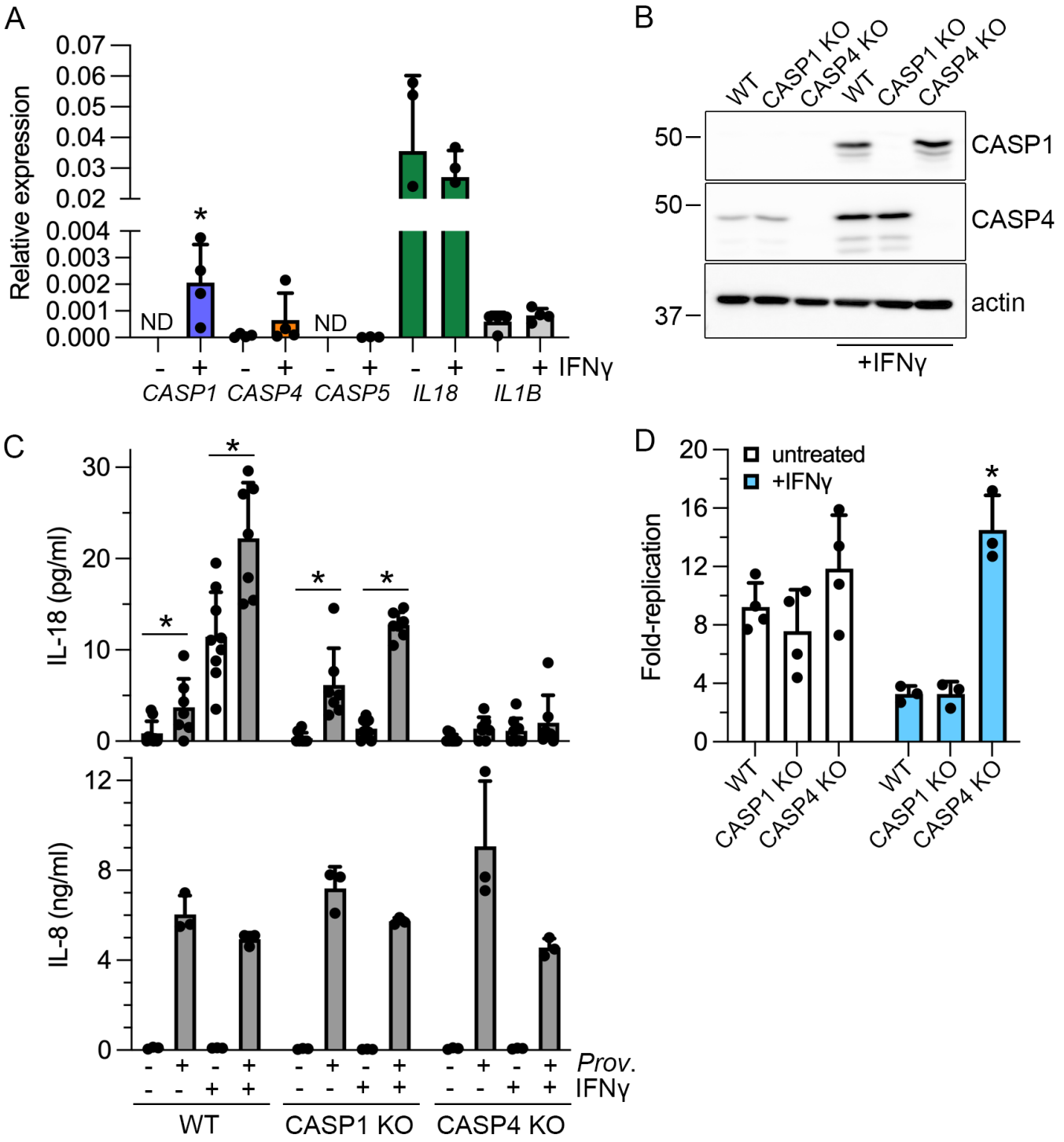

FIG 7 *P. alcalifaciens* 205/92 activates the non-canonical inflammasome in IECs. (A) HCT116 cells were left untreated or treated with 50 ng/mL IFNγ for 16–18 hours. mRNA expression of *CASP1*, *CASP4*, *CASP5*, *IL18,* and *IL1B* relative to the reference gene *RPLP0* was measured by qPCR (expressed as $2^{-\Delta Cq}$). *n* = three–four independent experiments. The asterisk indicates data significantly different from those of untreated cells, $P < 0.05$, Student's *t*-test. (B) Immunoblot analysis of caspase-1, caspase-4, and ß-actin (loading control) in HCT116 WT, *CASP1*$^{-/-}$ (CASP1 KO) or *CASP4*$^{-/-}$ (CASP4 KO) cells, left untreated or treated with IFNγ for 16–18 hours. (C) IL-18 (upper panel) and IL-8 (lower panel) release into supernatants from mock-infected or *P. alcalifaciens*-infected HCT116 WT, CASP1 KO, or CASP4 KO cells (MOI ~150) at 16 h p.i. was quantified by ELISA. $n \geq 8$ independent experiments. Cells were treated with IFNγ (50 ng/mL) for 16–18 hours before infection where indicated (+). Asterisks indicate significantly different data, $P < 0.05$, Student's *t*-test. (D) Bacterial replication in HCT116 WT, CASP1 KO, and CASP4 KO cells was assessed by gentamicin protection assay. Fold-replication is CFU_{10h}/CFU_{1h}. The asterisk indicates data significantly different from those of HCT116 WT, $P < 0.05$, ANOVA with Dunnett's *post-hoc* test. *n* = three–four independent experiments.

HTC116 cells upon IFNγ-priming (14.5-fold; Fig. 7D). In C2Bbe1 cells, enhanced bacterial proliferation was detected in *CASP4*$^{-/-}$ cells, irrespective of IFNγ priming (Fig. S3C). Therefore, caspase-4, but not caspase-1, restricts the intracellular proliferation of *P. alcalifaciens* in human IECs.

Infection models

We first used the bovine ligated intestinal loop model to assess the enteropathogenicity of *P. alcalifaciens* 205/92. We have previously used this infection model to study another enteric pathogen, *S*. Typhimurium (80). Bacteria (~10^9 CFU) were injected into each loop, and loops were collected at 12 hours post-inoculation. By CFU counts, most bacteria remained extracellular, with only 10^7 WT bacteria being tissue-associated (Fig. 8A). Compared to the LB control, infection with *P. alcalifaciens* 205/92 did not promote fluid accumulation in the calf model (Fig. 8B), a proxy for intestinal secretory responses. Infection-induced inflammatory changes were assessed by histological evaluation of hematoxylin- and eosin-stained sections of tissue samples. Of the six criteria scored —polymorphonuclear infiltration to the lamina propria, submucosal edema, epithelial damage, villus blunting, crypt abscess, and cell death (Table 1) —only epithelial damage was increased with statistical significance in infected tissues (P = 0.04, Student's *t*-test; Fig. 8C through E). In this infection model, we did not observe any difference in fluid or tissue colonization (Fig. 8F), fluid accumulation or local inflammatory responses (results not shown) when comparing infection with WT, Δ*invA*$_{1a}$, or Δ*invA*$_{1b}$ bacteria at 2 h or 8 h p.i.

As an alternative infection model, we used *D. melanogaster* to test whether T3SS$_{1a}$ or T3SS$_{1b}$ were required for virulence. In insect hosts, *P. alcalifaciens* is highly virulent (13). In previous studies, an infection dose of 10^3–10^4 Dmel, a *P. alcalifaciens* strain initially isolated from wild-type *D. melanogaster*, or ~3750 CFU *P. alcalifaciens* DSM30120, led to fly death in 1–2 days (13, 81). In our initial studies, an infection dose of ~300 CFU for *P. alcalifaciens* 205/92 proved too high, with rapid killing of all flies between 30 and 40 hours (results not shown). When we reduced the infection dose to 30 CFU, all flies succumbed to infection with WT bacteria within 45–68 hours (Fig. 9). Virulence of *P. alcalifaciens* Δ*invA*$_{1a}$ bacteria was comparable to that of WT bacteria at an infection dose of 30 CFU (Fig. 9, P = 0.83), whereas Δ*invA*$_{1b}$-infected flies showed an extended time to death (Fig. 9, P < 0.0001). *P. alcalifaciens*-induced mortality was dose-dependent; at a lower infectious dose of WT bacteria (10 CFU), 5%–6% of flies survived for up to 93 hours, when we stopped monitoring survival (Fig. 9). Compared to WT bacteria, we observed a prolonged time to death and decreased mortality during infection with Δ*invA*$_{1a}$ and Δ*invA*$_{1b}$ bacteria at a dose of 10 CFU (Fig. 9). Both survival curves were significantly different from infection with WT bacteria (P = 0.0019 for Δ*invA*$_{1a}$ and P < 0.0001 for Δ*invA*$_{1b}$), indicating that flies are less susceptible to infection with these gene deletion mutants. Overall, these results demonstrate two points: (1) flies are highly susceptible to infection with *P. alcalifaciens* 205/92 and (ii) T3SS$_{1a}$ and T3SS$_{1b}$ are both virulence determinants in an insect host.

DISCUSSION

T3SS play a central role in cell–cell interactions between bacteria and eukaryotes, irrespective of whether bacteria are pathogens, mutualists, or commensals (82). The high prevalence of T3SS in *Providencia* spp. suggests this supramolecular system is important for their colonization of specific ecological niches. Up to nine T3SS families have been identified in Gram-negative bacteria (83), and both T3SSs of *P. alcalifaciens* 205/92 belong to the Inv/Mxi-Spa family. Our earlier phylogenetic analysis of the translocator proteins in this family indicated that there are two sub-groups of T3SS (51). The first sub-group contains bacteria that colonize and cause disease in mammals, i.e., *S. enterica*, *S. flexneri*, enteroinvasive *E. coli* (EIEC), and *Chromobacterium* spp. *P. alcalifaciens* T3SS$_{1a}$ is also in this clade. The second sub-group, with T3SS$_{1b}$, contains bacteria that colonize diverse

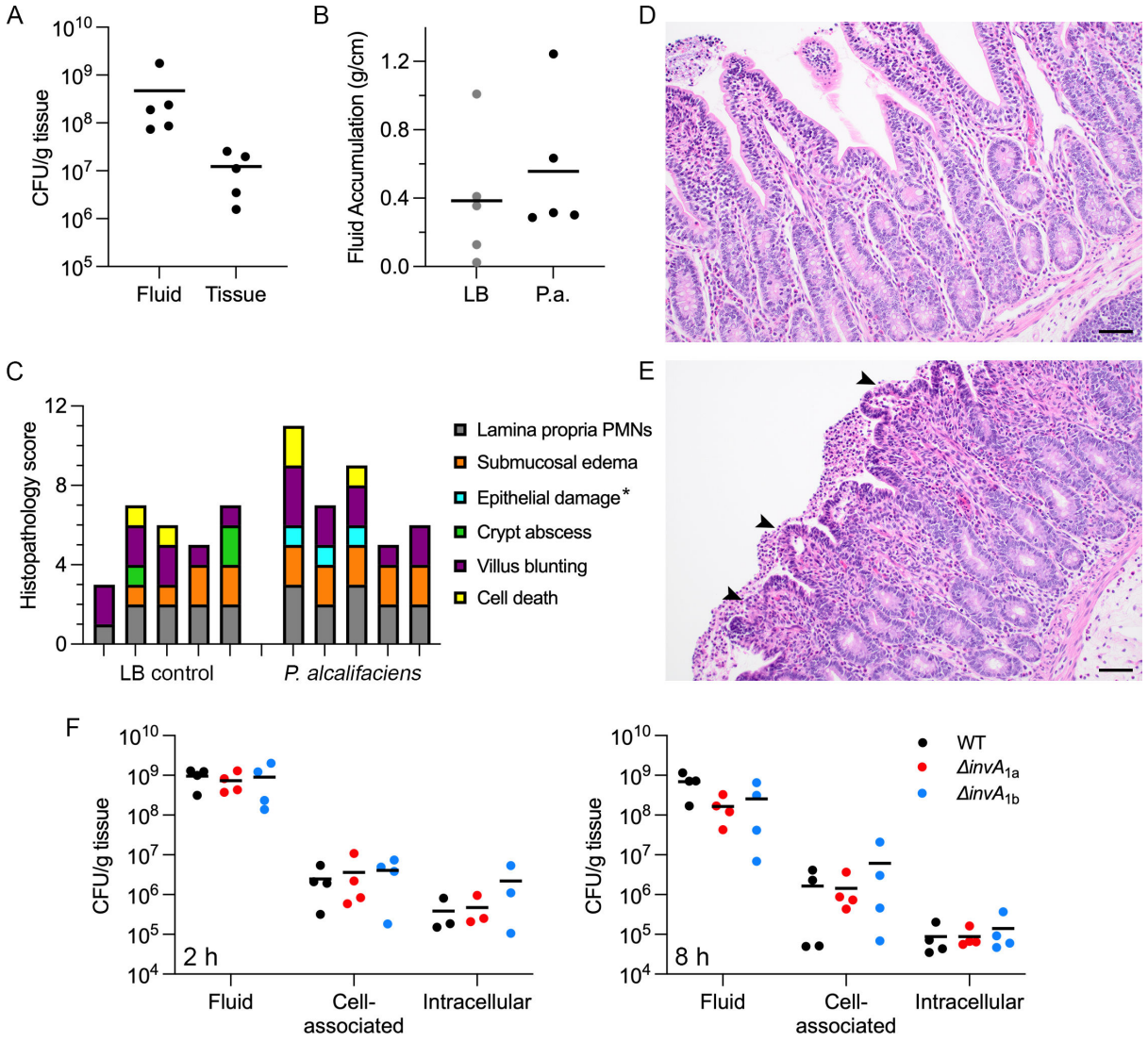

FIG 8 *P. alcalifaciens* 205/92 infection of bovine ligated intestinal loops. Bovine ligated intestinal loops were inoculated with LB broth (control) or *P. alcalifaciens* 205/92 (~10^9 CFU) resuspended in LB broth. (A) Recovery of WT bacteria from the fluid and tissue after 12 hours. Each dot represents data from one calf. Means are indicated. (B) Secretory responses in intestinal loops after infection with WT bacteria (P.a.) or LB control (LB) for 12 hours. Each dot represents data from one calf. Means are indicated. (C) Pathological scores from hematoxylin- and eosin-stained loop tissues sampled 12 hours after inoculation with LB broth or WT bacteria. *P. alcalifaciens* infection led to increased epithelial damage in the intestine (indicated by asterisk, $P = 0.040$, Student's *t*-test). Each vertical bar represents one calf. (D) and (E) Representative images (20 x objective) of hematoxylin- and eosin-stained sections of intestinal tissue from loops inoculated with LB broth alone (D) or WT bacteria (E) for 12 hours. Arrowheads indicate sites of epithelial damage. Scale bars are 50 µm. (F) Recovery of WT, Δ*invA*$_{1a}$, and Δ*invA*$_{1b}$ bacteria from the fluid and tissue (cell-associated or intracellular) after 2 hours (left panel) and 8 hours (right panel). Each dot represents the average of two–three loops per calf (2 hours) or one loop per calf (8 hours). Means are indicated.

environments, such as pathogens of fungi (*Pseudomonas gingeri*), plants (*Xanthomomas albilineans*), insects (*Providencia sneebia*), endosymbionts of insects (*Sodalis glossinidius*), and opportunistic pathogens of humans (*Proteus mirabilis*). Notably, T3SS required for bacterial colonization of insect hosts are restricted to the second sub-group. For example, the SSR-2 T3SS from *S. glossinidus* enhances bacterial proliferation in insect cells (52), the Ysa T3SS aids in *Y. enterocolitica* replication in insect, and not mammalian, cells (65), and PSI-2 from *Pantoea stewartii* is required for persistence in the gut of its flea beetle vector (84). We have further shown that T3SS$_{1b}$ is a *P. alcalifaciens* virulence factor in *D. melanogaster*. We predict that the T3SS$_{1b}$ from other *Providencia* spp., i.e., *P. sneebia*, *P. rettgeri,* and *P. vermicola* (19, 85, 86), will also promote insect infection.

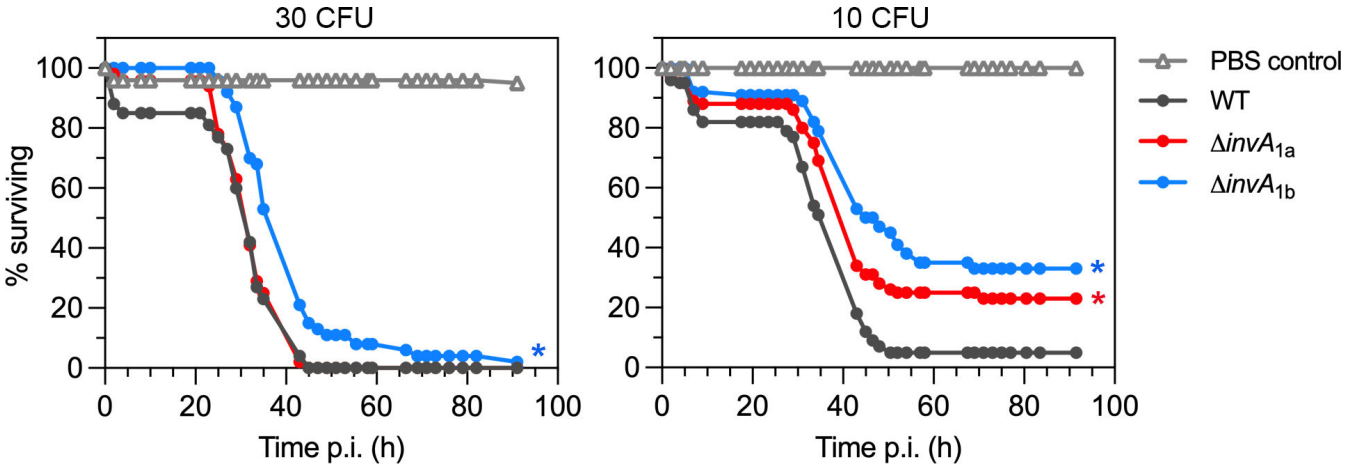

FIG 9 T3SS$_{1b}$, and to a lesser extent T3SS$_{1a}$, are virulence determinants in insects. *D. melanogaster* were inoculated with *P. alcalifaciens* 205/92 WT, Δ*invA*$_{1a}$, or Δ*invA*$_{1b}$ bacteria, or PBS, and survival was monitored. Results are from an infectious dose of ~30 CFU/fly (left panel) or ~10 CFU/fly (right panel) and are representative of two–three independent experiments. Asterisks indicate survival curves significantly different from WT infection ($P < 0.05$, logrank test). >50 flies were inoculated with PBS or each strain in each experiment.

The differential contribution of T3SS$_{1a}$ and T3SS$_{1b}$ to vertebrate and invertebrate host colonization, respectively, likely explains their distinct responses to environmental cues. *S.* Typhimurium T3SS1 and *P. alcalifaciens* T3SS$_{1a}$ genes are induced under similar *in vitro* conditions—late-log phase of growth, aeration, and high salt (60, 87)—and rapidly downregulated following bacterial internalization into eukaryotic cells (60), suggesting that they share commonalities in their regulatory networks. Indeed, *P. alcalifaciens* T3SS$_{1a}$ encodes for orthologs of *hilA*, *invF,* and *sicA* (Fig. 2A), three of the main transcriptional regulators of T3SS1 activity in *S.* Typhimurium (88). *In vitro* growth conditions that induce T3SS$_{1b}$ genes remain an enigma as altering the growth phase, temperature, pH, and nutrient availability was unsuccessful. We also did not observe T3SS$_{1b}$ gene induction upon bacterial infection of mammalian (HCT116) or insect (S2) cells. However, the Δ*invA*$_{1b}$ deletion mutant is attenuated in flies, which indicates there are gene induction cues in the insect model that we have not been able to recapitulate in broth or tissue culture cells. T3SS$_{1b}$ encodes for *invF* and *sicA* orthologs, but interestingly, no *hilA* ortholog is present in this pathogenicity island (Fig. 2A) or elsewhere on the chromosome. Overall, our data support the idea that *P. alcalifaciens* extended its host range from the natural environment to living organisms by acquiring these two divergent T3SS, each adapted to a target host class: *Mammalia* (T3SS$_{1a}$) or *Insecta* (T3SS$_{1b}$).

Gram-negative bacteria in the genus *Providencia* are considered opportunistic pathogens. *P. alcalifaciens* is part of the human gut microbiome (8) and has been isolated from the feces of healthy people and animals (21, 29, 39, 89) and from wastewater treatment plants (90). *P. alcalifaciens* is also an enteropathogen (31, 32, 39, 40). Based on the available genome sequences and strain source details, we describe a strong link between the subset of *P. alcalifaciens* strains that harbor T3SS$_{1a}$ (Fig. 1) and those that cause diarrheal disease in dogs (e.g., strains 2019–04-29292-1-3 and 2019004029290-1-7; Table S1) and humans (e.g., strains 205/92, 2939/90 and RMID 1656011; Table S1). Therefore, it seems that the acquisition of genes encoding a second T3SS on a large plasmid has contributed to the emergence of enteropathogenic *P. alcalifaciens* strains (45, 91). Also encoded on the 128-kb plasmid of *P. alcalifaciens* 205/92 are homologs of type III effectors known to be bacterial virulence determinants in mammalian hosts, including SptP, EspG, EspM, SipA$_{1a}$, and VopT. SptP from *S. enterica* has two distinct functions. Its tyrosine phosphatase activity interferes with extracellular-regulated kinase (ERK) MAP kinase pathways in the host cell (92). It also acts as a GTPase activating protein (GAP) for Rac1 and Cdc42 to reverse actin cytoskeletal changes that accompany bacterial entry into epithelial cells (93). The EspG protein family consists of EspG/EspG2

and VirA (94). EspG from enteropathogenic *E. coli* (EPEC) disrupts the host cell secretory pathway (95). VirA is required for efficient entry of *Shigella* into epithelial cells and intra- and inter-cellular bacterial spread (96). The EspM/Map/IpgB2 family of effectors are found in EPEC, EHEC, and *Shigella* and modulate actin dynamics (97). *S. enterica* SipA and *S. flexneri* IpaA are functional orthologs that induce a loss of actin stress fibers to promote bacterial entry into non-phagocytic cells (98, 99). In addition to its actin-binding role, SipA is necessary and sufficient for polymorphonuclear leukocyte (PMN) migration across the intestinal epithelium *in cellulo* and *in vivo* (100). Of interest, the molecular mass of $SipA_{1a}$ from a subset of *P. alcalifaciens* strains (e.g., strains 205/92, 2939–90, 2019–04-28369-1-2, 2019–04-29292-1-3, 2019–04-29034-1-3, 2019–04-2920-1-7, 2019–04-27799-1-2, and 2019–04-3283-1-1; Fig. 1 and 2) is unusually large compared to that of SipA from *S. enterica*, IpaA from *S. flexneri*, or CipA from *C. violaceum*. This is due to an extended C-terminus (Fig. 1B); the biological function of this $SipA_{1a}$ domain is unknown. VopT from *Vibrio parahaemolyticus* is a type III translocated toxin that ADP-ribosylates the Ras protein (101). p128kb also encodes for a TcdA/TcdB-type toxin, an exotoxin best characterized in *Clostridioides difficile* (102). Additionally, the chromosome of *P. alcalifaciens* 205/92 encodes for homologs of known type III effectors including SteB and SteC from *S.* Typhimurium and a second SipA ($SipA_{1b}$). SteB contributes to *S.* Enteritidis biofilm formation on plastics (103), but the role of SteB in *Salmonella*–eukaryotic cell interactions has not yet been deciphered (104). SteC is a kinase that promotes actin cytoskeleton reorganization around the *Salmonella*-containing vacuole (105, 106). Theoretically, this type III effector repertoire would allow *P. alcalifaciens* to enter and proliferate within eukaryotic cells. We are currently investigating whether these are *bona fide* type III effectors and if there are additional type III effectors of *P. alcalifaciens*.

We report that *P. alcalifaciens* 205/92 rapidly and efficiently lyses its internalization vacuole in mammalian and insect cells and then proliferates in the eukaryotic cell cytosol. A previous study showed that *P. alcalifaciens* 101i/59, an invasive isolate, was enclosed within vacuoles and present in the cytosol of Caco-2 cells at 4–6 h p.i. using crystal violet staining (49). Another invasive isolate, 82 A-5778, occupied vacuoles "in close proximity to the nuclear membrane" and the cytosol in Hep-2 cells (46). However, no quantification of vacuolar versus cytosolic residence was provided in these two studies. We speculate that all *P. alcalifaciens* isolates that harbor $T3SS_{1a}$ adopt a cytosolic lifestyle inside eukaryotic cells. We further identified mammalian cell responses that are indicative of host sensing of cytosolic bacteria, namely, activation of the caspase-4 (non-canonical) inflammasome, followed by inflammatory cytokine release upon *P. alcalifaciens* infection of IECs. Caspase-4 also limits the cytosolic proliferation of *P. alcalifaciens*; whether this is via pyroptotic cell lysis is unknown. There is no evidence for caspase-1-dependent host responses to *P. alcalifaciens* in colonic epithelial cells, which is in line with studies of other enteric pathogens in human IECs (78, 79).

In addition to inflammasome activation, ubiquitin-mediated autophagy is also an important host innate defense against cytosolic bacteria. Here, we describe that nascent vacuole lysis is partially dependent on $T3SS_{1a}$ in human IECs, but not human macrophages or insect cells (Fig. 6), indicating host- and cell-type differences in *P. alcalifaciens* disruption of the surrounding vacuole membrane. Failure of $\Delta invA_{1a}$ bacteria to efficiently lyse the nascent vacuole in IECs results in bacterial killing (Fig. 4). This hints that type III effectors are involved in disrupting the internalization vacuole membrane and preventing the autophagic recognition of *P. alcalifaciens* in human IECs. Orthologs of type III effectors known to interfere with autophagic recognition (e.g., VirA and IcsB in *S. flexneri*, SopF in *S.* Typhimurium, and TssM in *Burkholderia* spp.) are not present in the genome of *P. alcalifaciens* 205/92, however. Other known mechanisms used by bacteria to deflect targeting by selective autophagy are LPS and O-antigen modifications (107, 108), enzymatic modification of bacterial outer membrane proteins (108), and bacterial phospholipase manipulation of host cell phospholipids (109–111). Our research efforts are currently directed toward defining how *P. alcalifaciens* mediates vacuolar escape and resists autophagic detection in mammalian cells.

Prior to our work, rabbits and suckling mice were the two animal models used to study the enteropathogenesis of *P. alcalifaciens* infection. Murata *et al*. (31) studied the secretory and inflammatory responses to *P. alcalifaciens* clinical isolates from a foodborne outbreak in Japan in rabbit ileal loops (31). Histopathological analysis of loops infected with one of these isolates (RIMD1656011) showed extensive mucosal inflammation including neutrophil infiltration within the lamina propria and distortion of the villus architecture. Seven isolates caused a moderate level of fluid accumulation after 20 hours. By contrast, three isolates from diarrheal patients, one isolated in Bangladesh (2939/90) and two in Australia (F90-2004, R90-1475), failed to induce fluid accumulation in the rabbit ileal loop assay after 20 hours (40). Likewise, four *P. alcalifaciens* isolates from a foodborne outbreak in Kenya did not induce fluid accumulation in rabbit ileal loops over 18 hours in a third study (33). In a suckling mouse model (42), one *P. alcalifaciens* strain (AH-31) caused diarrhea in 7 of 12 mice, while another (AS-1) did not cause diarrhea in any mice. As an alternative animal model, we considered calves because they are a relevant model for the study of enteric disease associated with human salmonellosis. Published literature indicates *Providencia* spp. are associated with cattle; antimicrobial-resistant *Providencia* spp. have been isolated from cow manure (112), feces- and urine-contaminated bedding from yearling calf pens (113), and raw cow's milk (114), and *P. stuartii* causes neonatal diarrhea in dairy cows (115). In our studies, fluid accumulation was not observed in calf intestinal loops that were exposed to *P. alcalifaciens* 205/92 for 12 hours. Histopathological analysis of infected loops also did not show indicators of an acute inflammatory reaction, but mild epithelial damage was observed. Collectively, these studies suggest that either *P. alcalifaciens* causes non-inflammatory diarrhea, or intestinal loops in rabbits and calves are not an appropriate animal model to study the enteropathogenic properties of this bacterium. It should be noted, however, that the RITARD infection model, which was developed in the early 1980's to study *Vibrio cholerae* and enterotoxigenic *E. coli* enteric infections (116), supports the diarrheagenic nature of *P. alcalifaciens* clinical isolates (40).

Providencia spp. have been isolated from the hemolymph of wild-caught *D. melanogaster* (13) and as part of the gut microbiome in *Bactrocera dorsalis*, the Oriental fruit fly (117), but it is not known if these bacteria are intracellular in insects. Fruit flies are exquisitely sensitive to infection by *P. alcalifaciens* (our results (13, 81)). In *D. melanogaster* infections, *P. alcalifaciens* proliferates rapidly, reaching bacterial loads of ~10^7–10^8 CFU per fly by 20–32 h p.i (13, 81). Flies die shortly after (our results (13, 81)). On the host side, Imd-dependent antimicrobial peptides and hemocyte-derived reactive oxygen species are the major branches of insect immunity that are important for fighting infection with *P. alcalifaciens* (81). In a forward genetics screen using a *P. alcalifaciens* DSM30120 transposon mutant library, lipopolysaccharide (LPS) and lipoprotein mutants showed reduced virulence in *D. melanogaster* (81). Even though DSM30120 encodes for $T3SS_{1b}$ (but not $T3SS_{1a}$; Fig. 1C; Table S1), no bacterial mutants in toxins or the T3SS were hit in this screen (81). By contrast, we identified that $T3SS_{1b}$, and to a lesser extent $T3SS_{1a}$, are virulence factors in *D. melanogaster* (Fig. 9), which is the first report of *P. alcalifaciens* T3SSs being virulence determinants in insects. We believe that the different results might be explained by the much lower infection dose used in our study (10–30 CFU vs 1,500 CFU). Considering their high prevalence among *Providencia* spp. genomes (50), our results suggest that T3SSs are a widespread pathogenicity factor for invertebrate colonization by members of this genus. Furthermore, insects have a well-known role in transmitting clinically relevant pathogens, and *Providencia* spp. are often resistant to multiple antimicrobials, so studying the insect carriage of bacteria such as *P. alcalifaciens* may provide information about the role that invertebrate hosts play in the maintenance and transmission of antimicrobial resistance.

While historically viewed as opportunistic pathogens, the *Morganella–Proteus–Providencia* (MPP) group of organisms (*Morganella morganii*, *Proteus vulgaris, and Providencia* species) are increasingly being recognized as emerging causes of multidrug-resistant infections because of inducible chromosomal β-lactamases and a propensity to acquire

other resistance determinants. The genomic plasticity of *Providencia* spp. is noteworthy, and can be seen in the varied lifestyles of different species and strains, ranging from commensal residents of the gastrointestinal tract to assorted pathogens that promote intestinal or extraintestinal illnesses with different clinical consequences. Whole-genome sequencing has provided considerable information about the genomes of non-pathogenic and pathogenic *P. alcalifaciens* and what genes might contribute to the pathogenicity of this bacterial species (50, 118). From our work, and that of others, it is evident that some *P. alcalifaciens* strains have gained the ability to enter and proliferate within mammalian cells and cause damage to the gut epithelium and subsequent diarrheal disease. Acquisition of an "invasion-associated" plasmid drove this evolutionary leap. Altogether, our work argues that the importance of *P. alcalifaciens* as a *bona fide* enteropathogen should not be ignored and supports its inclusion into systematic surveillance programs.

MATERIALS AND METHODS

Bacterial strains and plasmid construction

P. alcalifaciens 205/92 (Tet^R) served as the WT strain and background for deletion mutants in this study. It was initially isolated from the stool of a 12-year-old boy with watery diarrhea (43). Allelic exchange with a counter-selectable suicide vector harboring *sacB* (pRE112; Cm^R (119)) was used to generate in-frame deletions of $invA_{1a}$ and $invA_{1b}$. Deletion cassettes were amplified from *P. alcalifaciens* 205/92 genomic DNA by overlap extension PCR using oligonucleotides listed in Table S2 and ligated into pRE112. The resulting plasmids were electroporated into *E. coli* SY327λpir for sequence confirmation, then transferred by electroporation into *E. coli* SM10λpir (Kan^R), followed by conjugation into *P. alcalifaciens* 205/92 WT (Tet^R). Selection of conjugants was on LB agar containing tetracycline (10 µg/mL) and chloramphenicol (30 µg/mL). The resulting meridiploids were counter-selected by incubating overnight on LB agar containing 1% (wt/vol) tryptone, 0.5% (wt/vol) yeast extract, and 5% (wt/vol) sucrose at 30°C. Sucrose-resistant clones were screened by PCR using primers flanking the recombination region to verify gene deletions. For *in trans* complementation of Δ$invA_{1a}$, the upstream regulatory region of $invF_{1a}$ was fused to the open reading frame of $invA_{1a}$ by overlap extension PCR using the oligonucleotides listed in Table S2 with *P. alcalifaciens* genomic DNA. The resulting amplicon was then ligated into the *Bam*HI/*Xma*I sites of pGEN-MCS (120) to generate pGEN-$invA_{1a}$, which was then electroporated into *P. alcalifaciens* Δ$invA_{1a}$ bacteria. For fluorescence detection of *P. alcalifaciens*, bacteria were electroporated with pGEN-DsRed (121), which encodes for the red fluorescent protein variant, DsRed.T3, under the control of the *em7* promoter.

To generate transcriptional reporters for genes associated with $T3SS_{1a}$, $T3SS_{1b}$, and flagella, predicted promoter regions of putative regulators or structural components were amplified with oligonucleotides listed in Table S2 and cloned into pFU35 (122) upstream of the *luxCDABE* operon. Sequence-confirmed reporter plasmids were electroporated into *P. alcalifaciens* WT bacteria. Plasmid stability of the pFU series of fusion vectors has been confirmed in *E. coli*, *S.* Typhimurium, and *Yersinia pseudotuberculosis*; in the absence of antibiotic selection, >95% of bacteria retained the plasmids for up to 6 days in liquid culture (122). We expect similar levels of plasmid stability in *P. alcalifaciens* over the experimental time frames we are using (12 hours in broth and 6 hours in tissue culture cells).

S. Typhimurium SL1344 was the wild-type strain used in this study (123). The *S.* Typhimurium SL1344 translocator swap mutants, Δ*sipC::PasipC*$_{1a}$ and *sipC::cipC*, have been described previously (51).

Bacterial genome sequencing and assembly

A log-phase culture of *P. alcalifaciens* 205/92 was centrifuged, and the bacterial pellet was resuspended in 1 x DNA/RNA Shield (Zymo). Bacterial DNA was extracted and sequenced at Plasmidsaurus Inc. (Eugene, Oregon) using Oxford Nanopore Technologies (v14 library prep chemistry, R10.4.1 flow cell, base-called using dna_r10.4.1_e8.2_5 khz_400bps_sup@v4.2.0 model, and primer- and adapter-trimmed) and Illumina (NextSeq 2000, 153-bp paired-end reads). Raw sequencing reads were deposited to ENA (BioProject PRJNA1100810). Raw Illumina reads were adapter- and quality-trimmed using bbduk.sh v38.07, using options "ktrim = r k = 23 mink = 11 hdist = 1 tpe tbo." Nanopore reads were filtered using filtlong v0.2.1 against the trimmed Illumina reads, with options "--min_length 1000 --keep_percent 90 --target_bases 500000000 –trim --split 500," selecting approximately 100 x coverage of best Nanopore reads. All scripts used in the analysis can be found in https://github.com/apredeus/P_alcalifaciens.

Resulting filtered Nanopore reads were assembled using Trycycler v0.5.4, which uses manual curation of long-read assemblies to achieve a nearly perfect bacterial genome assembly. To this end, raw Nanopore reads were randomly subsampled to 50 x depth and assembled 10 times each using the following long-read assemblers: flye v2.9.2-b1786, raven v1.8.1, and miniasm 0.3-r179. Following this, 25 assemblies (nine flye, eight raven, and eight miniasm) were selected for further analysis. Assembled contigs were clustered and evaluated; three supported clusters were retained, outlier contigs in each cluster were removed, and reconciled sequences generated. Additionally, Unicycler v0.5.0 was run in the hybrid mode on both Nanopore and Illumina reads to recover small plasmids that long-read approaches could potentially miss because of size selection bias. This allowed the recovery of a small (~4 kb) plasmid missed by long-read-only assembly.

The final assembly consisted of one chromosome and three plasmids. The chromosome was rotated to match the start of RefSeq assembly GCF_002393505.1 (strain FDAARGOS_408, representative *P. alcalifaciens* genome). Following this, polishing with the trimmed Illumina reads using Polypolish v0.5.0 (124) was done to correct the remaining small indels and single-nucleotide polymorphisms. The resulting assembly was submitted to the NCBI (GenBank Accession No. GCA_038449115.1). To annotate the genome, Bakta v1.9.1 was run with settings "--complete --compliant --genus Providencia --species alcalifaciens --locus-tag PA205 --keep-contig-headers." To annotate candidate prophage regions, PHASTER online service (https://phaster.ca/, accessed on 15th March, 2024) was used together with the manual curation using individual protein annotations from Bakta.

For the comparative genome analysis, all of the *P. alcalifaciens* genome assemblies available via Genbank on 10th March 2024 were downloaded as finished assemblies; entries marked as anomalous by the NCBI were excluded. Additionally, representative genomes of *P. rustigianii* (strain 52579_F01, assembly GCA_900637755.1) and *P. rettgeri* (strain AR_0082, assembly GCA_003204135.1) were downloaded to be used as potential outgroups. In total, 51 assemblies were downloaded; of these, 13 were marked as "Complete genome," 28 were marked "Contig," and another eight were marked "Scaffold" (Table S1). Using snippy v4.6.0 in the contig mode, and our assembly of strain 205/92 as a reference, all other assemblies were mapped and variant-called. Assemblies were evaluated for quality, and assemblies with more than 60% of the reference genome covered were removed (Table S1). Following this, snippy-core utility v4.6.0 was used to create core genome alignment of the remaining genomes.

Pairwise SNP distances were calculated using snp-dist v0.8.2 using the AGCT-only core genome alignment. Constant sites in the full core genome alignment were identified using snp-sites v2.5.1. To determine the plasmid coverage, *in silico* reads generated by Snippy from assembled contigs (single-end, 250 bp) were mapped to our assembly of *P. alcalifaciens* strain 205/92 using bwa v0.7.17-r1188, and samtools v1.18 "coverage" command was used to calculate the coverage of individual plasmids. Plasmids

with >80% coverage were classified as fully present; plasmids with 40%–80% coverage were classified as partially present.

IQTree v2.2.4 was run using constant sites defined above, and with the options "-redo -ntmax 16 -nt AUTO -st DNA -bb 1000 -alrt 1000." The best-fit model was selected by the Bayesian information criterion. The resulting tree, plasmid presence, and SNP distances were visualized using R 4.3.3 with packages ggtree (v3.10.1), treeio (v1.26.0), tidytree (v0.4.6), and pheatmap (v1.0.12).

BRIG v0.95 and NCBI blast 2.7.1+ were used to align and produce the circular visualization of the chromosome and the largest plasmid. To be used in BRIG, all of the multi-fasta genome assemblies were converted to a single fasta using a custom script. All scripts used for the analysis and visualization are available at https://github.com/apredeus/P_alcalifaciens.

Bacterial growth curves

P. alcalifaciens was grown overnight in LB–Miller broth (Difco) for 16–18 hours with shaking (220 rpm) at 37°C. Cultures were back-diluted into 10 mL LB–Miller broth in a 125-mL Erlenmeyer flask to a starting optical density at 600 nm (OD_{600}) of 0.1 and grown with aeration (220 rpm) at 37°C. OD_{600} was measured hourly in a BioRad SpartSpec Plus spectrophotometer.

Bacterial luminescence

Bacteria were subcultured as described above for 12 hours. Each hour, 150 µL of the subculture was transferred, in duplicate, to a white flat-bottom 96-well polystyrene microplate (Corning Costar) sealed with polyester Axyseal film (Axygen Inc.). Luminescence was measured using a Tecan Infinite M1000 plate reader.

For quantification of bacterial luminescence upon infection of mammalian and insect cells, cells were seeded in 6-well plates: (1) HCT116 cells at 4×10^5 cells/well on rat tail collagen ~40–44 hours prior to infection (2); S2 cells at 2×10^6 cells/well ~ 24 hours prior to infection. Infections with *P. alcalifaciens* subcultures were as described below. At the required time point, infected monolayers were washed twice with Hanks' balanced salt solution (HBSS, Corning), collected in 1 mL sterile double-distilled water using a cell scraper (Sarstedt), transferred to a 1.5-mL Eppendorf tube, vortexed, and then centrifuged at 8,000 x *g* for 2 minutes to pellet bacteria. The supernatant was carefully removed and discarded, and the pellet was resuspended in 100 µL PBS and transferred to a white flat-bottom 96-well polystyrene microplate (Corning Costar). Luminescence was measured using a Tecan Infinite M1000 plate reader.

Motility assays

Overnight cultures of *P. alcalifaciens* 205/92 WT, *S*. Typhimurium SL1344 WT, and Δ*flgB* mutant (60) were inoculated into the center of Petri dishes containing LB plus 0.3% (wt/vol) agar using a sterile pipette tip, piercing approximately half-way through the semi-solid agar. Plates were incubated overnight at 37°C.

Secretion assays and mass spectrometry

Two 10 mL subcultures were grown for 4 hours with shaking for each strain, as described above, and pelleted for 15 minutes at 16,000 x *g*. Supernatants were pooled and filtered with a 0.22-µm low-protein binding Acrodisc filter (Whatman). Proteins were precipitated in 10% (wt/vol) trichloroacetic overnight at 4°C. Protein precipitates were collected by centrifugation at 16,000 x *g* for 15 minutes at 4°C, and pellets were washed with cold acetone, dried, and resuspended in 200 µL 1.5X SDS-PAGE sample buffer. Secreted proteins were separated on a 10% SDS-PAGE gel and visualized by Coomassie Brilliant Blue stain (Fisher). For protein identification, secreted proteins were separated on 4%–15% gradient SDS-PAGE gels (BioRad), stained with GelCode Blue (Thermo), and bands of interest were excised and sent to Stanford University Mass Spectrometry (SUMS) facility

for protein identification by LC/MS/MS. Following in-gel tryptic digestion, reconstituted samples were analyzed using a nanoAcquity UPLC (Waters) coupled to an Orbitrap Q-Exactive HF-X (RRID:SCR_018703) mass spectrometer.

Tissue culture

HCT116 cells (human colorectal carcinoma epithelial), HeLa (human cervical carcinoma), THP-1 (human monocytes), and J774A.1 (mouse macrophage-like) cells were purchased from ATCC and used within 15 passages of receipt. HCT116 cells were maintained in McCoy's medium 5A (Iwakata and Grace Modification, Corning), supplemented with 10% (vol/vol) heat-inactivated fetal calf serum (FCS, Invitrogen). HCT116 *CASP1*$^{-/-}$ and *CASP4*$^{-/-}$ knockout (KO) cells were generated using CRISPR-Cas9 technology by Synthego (www.synthego.com). *CASP1*$^{-/-}$ KO clones G15 and I17 and *CASP4*$^{-/-}$ KO clones J3 and N8 were derived by single-cell expansion. Premature termination of the respective genes was verified by DNA sequencing. *CASP1*$^{-/-}$ KO (clone 1.5) and *CASP4*$^{-/-}$ KO (clone 4.15) Caco-2 C2Bbe1 cells (human colorectal adenocarcinoma) and the parental wild-type (WT) cells were provided by Dr Jason Smith (University of Washington) and have been described previously (79). C2BBe1 cells were grown in Dulbecco's modified Eagle medium (DMEM, 4.5 g/L glucose, Corning) containing 4 mM L-glutamine, 10 µg/mL human transferrin (Sigma), and 10% (vol/vol) heat-inactivated FCS. Where indicated, HCT116 and C2Bbe1 cells were treated with IFNγ (PeproTech) at 50 ng/mL for 16–18 hours. HeLa cells were maintained in Eagle's minimal essential medium (Corning) containing 2 mM L-glutamine, 1 mM sodium pyruvate, and 10% (vol/vol) heat-inactivated FCS. THP-1 cells were maintained in RPMI 1640 medium (Corning) containing 1 mM sodium pyruvate, 2 mM L-glutamine, 10 mM HEPES, and 10% (vol/vol) heat-inactivated FCS. J774A.1 cells were maintained in DMEM containing 4 mM L-glutamine and 10% (vol/vol) heat-inactivated FCS. All mammalian cell lines were maintained at 37°C in 5% CO_2. *Drosophila S2* cells were purchased from Invitrogen and used up to passage number 20. Cells were maintained in Schneiders' medium (Invitrogen) with penicillin–streptomycin and 10% (vol/vol) heat-inactivated FCS. S2 cells were maintained at 26°C without CO_2. Cells were seeded in 24-well tissue culture-treated plates (Nunc) at the following densities: (i) HCT116 and C2Bbe1, 1×10^5 cells/well ~ 44 hours prior to infection on rat tail collagen (Corning), and growth medium was changed on C2Bbe1 cells to transferrin-free media 4 hours prior to infection, (ii) HeLa, 5×10^4 cells ~24 hours prior to infection, (iii) THP-1, 2.5×10^5 cells/well ~ 48 hours prior to infection in the presence of 200 nM phorbol 12-myristate 13-acetate (PMA, LC Laboratories), and growth medium was replaced with PMA-free media 4 hours prior to infection, (iv) J774A.1, 2×10^5 cells/well ~ 24 hours prior to infection, (iv) S2, 5×10^5 cells/well ~ 24 hours prior to infection, and growth medium was changed to penicillin–streptomycin-free media 4 hours prior to infection.

Gentamicin protection and CHQ resistance assays

To enumerate intracellular bacteria, cells were seeded and infected as described above and subject to a gentamicin protection assay as described (68). *P. alcalifaciens* strains were subcultured for 3.5–4 hours as detailed above. One mL of subculture was pelleted at 8,000 x *g* for 90 seconds, resuspended in 1 mL HBSS (Corning), and diluted 1:100 in HCT116 or C2Bbe1 growth media (transferrin-free) or 1:1000 in THP-1 or S2 growth media. Because *P. alcalifaciens* are poorly motile (Fig. S2), we centrifuged late log-phase cultures onto host cells to promote bacteria–host cell association, a technique typically used for nonmotile or poorly motile bacteria (60, 62, 67). Without this centrifugation step, no *P. alcalifaciens* were internalized into non-phagocytic (HCT116) cells after 30 minutes of co-incubation (our unpublished results). One milliliter of the diluted culture was centrifuged onto cells at 500 x *g* for 5 minutes at room temperature (t_0) (multiplicity of infection (MOI) of ~150 for HCT116 and C2Bbe1, ~10 for THP-1, and ~5 for S2), and then monolayers were incubated for a further 25 minutes at 37°C (HCT116, C2Bbe1, and THP-1) or 26°C (S2). Extracellular bacteria were removed at 30 min p.i. by washing

three times with 1 mL HBSS and then incubated in growth media containing 100 µg/mL gentamicin at 37°C (HCT116, C2Bbe1, and THP-1) or 26°C (S2). At 1 h p.i., monolayers were washed once with 1X PBS and solubilized in 0.2% (wt/vol) sodium deoxycholate (NaDOC). Internalized bacteria and subculture inocula were serially diluted and plated on LB agar for CFU enumeration. Invasion efficiency was quantified as the number of internalized bacteria/inoculum x 100%. To measure intracellular replication over time, the multiplicity of infection (MOI) for the Δ*invA*$_{1a}$ mutant was increased by two- to threefold for HCT116 infections (MOI of 300–600) so that an approximately equivalent number of WT and Δ*invA*$_{1a}$ bacteria were internalized at 1 h p.i. Increasing the MOI of Δ*invA*$_{1a}$ bacteria up to tenfold did not compensate for its invasion defect in S2 cells, however. Media containing 100 µg/mL gentamicin was added from 30 to 90 min p.i. and then replaced with media containing 10 µg/mL gentamicin for the remaining time. Monolayers were solubilized at 4 , 8 , and 12 h p.i., serially diluted and plated as described above.

To determine the proportion of intracellular bacteria in the cytosol of eukaryotic cells, the CHQ resistance assay was used as previously published (67, 68). The concentration of CHQ was 400 µM for all cell types.

Inside/outside microscopy assay

Extracellular and intracellular bacteria were distinguished by staining with anti-*P. alcalifaciens* antibodies in the absence of any permeabilizing agents. Cells were seeded on acid-washed 12-mm-diameter glass coverslips (#1.5 thickness, Fisherbrand) in 24-well plates and infected with *P. alcalifaciens* WT, Δ*invA*$_{1a,}$ or Δ*invA*$_{1b}$ bacteria carrying pGEN-DsRed.T3. At 1 h and 8 h p.i., monolayers were fixed in 2.5% paraformaldehyde at 37°C for 10 minutes and then washed thrice in PBS. Extracellular bacteria were labeled with rabbit polyclonal anti-*P. alcalifaciens* antibody (kindly provided by Dr M. John Albert) diluted 1:250 in PBS containing 10% (vol/vol) normal goat serum (PBS-NGS; Invitrogen) for 15 minutes at room temperature. Monolayers were washed thrice in PBS, once in PBS-NGS, and then incubated with goat anti-rabbit Alexa-Fluor 488 secondary antibodies (Invitrogen) diluted 1:300 in PBS-NGS at room temperature for 15 minutes (150 µL per well). After three washes in PBS, host cell nuclei were labeled with Hoechst 33342 for 1 minute (Invitrogen, 1:10,000 dilution in water) and coverslips mounted in Mowiol (Calbiochem) on glass slides. Samples were viewed on a Leica DM4000 upright fluorescence microscope. A bacterium was scored as extracellular if it fluoresced red and green, or intracellular if it fluoresced red only.

Electron microscopy

SEM and TEM sample preparation and imaging was performed at the Franceschi Microscopy and Imaging Center at Washington State University using standard techniques. For SEM, HeLa and HCT116 cells were seeded on Thermanox plastic coverslips (Nunc), infected with *P. alcalifaciens* as described above, and at 20 min p.i. washed once in HBSS and fixed in 2% paraformaldehyde/2% glutaraldehyde in 0.1 M cacodylate buffer pH 7.2. overnight at 4°C. Glutaraldehyde-fixed cells were dehydrated in an ethanol series and dried at the critical point in CO_2. The samples were sputter coated with platinum/palladium to 2.5 nm thickness and examined on an FEI Quanta 200F scanning electron microscope.

For TEM, HeLa cells were seeded at 2×10^5 cells/well in 6-well plates the day before infection; HCT116 cells were seeded on rat tail collagen at 4×10^5 cells/well in 6-well plates ~ 40 hours prior to infection; THP-1 cells were seeded in the presence of PMA at 1×10^6 cells/well in 6-well plates 2 days prior to infection; S2 cells were seeded at 2×10^6 cells/well in 6-well plates. Monolayers were infected with *P. alcalifaciens* as described above and at 60–90 min p.i. gently washed thrice with PBS and treated with 0.25% trypsin (Corning) to detach HCT116 and HeLa cells or TrypLE Select (Gibco) to dislodge THP-1 cells. S2 cells were dislodged with a cell scraper (Sarstedt). Cells were collected,

centrifuged at 400 x *g* for 5 minutes, the supernatant discarded, and the cell pellet gently resuspended in fixative. Processing and imaging were done as described previously (66).

Cytotoxicity assays

Prior to infection, the medium was replaced on HCT116 cells and THP-1 cells to phenol-red free RPMI1640 (Corning) containing 10% (vol/vol) heat-inactivated FCS. Infections and subsequent steps were carried out in phenol-red free media. Cells were infected as described above, and supernatants were collected at the indicated times and centrifuged at 500 x *g* for 5 minutes to pellet cellular debris. Cell-free supernatants were collected and stored at −80°C until analysis. LDH release into the supernatant, a measure of the loss of plasma membrane integrity, was quantified using the Cytotox96 Assay Kit (Promega) according to the manufacturer's instructions.

Cytokine quantification by ELISA

HCT116 culture supernatants were collected at the indicated times, centrifuged at 500 x *g* for 5 minutes, and then the cell-free supernatants were stored at −80°C until analysis. IL-18 was quantified by sandwich ELISA as previously described (69). Mouse anti-human IL-18 monoclonal (125–2H) and rat anti-human IL-18 monoclonal (159–12B) biotin were purchased from MBL. Human IL-8 was quantified by DuoSet ELISA (R&D Systems) as per the manufacturer's instructions.

Immunoblotting

For analysis of whole cell lysates, adherent cells were washed twice in PBS prior to lysis in boiling 1.5 x SDS-PAGE sample buffer. Proteins were separated by SDS-PAGE and transferred to 0.45-µm pore-size nitrocellulose membranes (GE Healthcare Life Sciences). Membranes were blocked at room temperature for 1 hour with Tris-buffered saline (TBS) containing 5% (wt/vol) skim milk powder and 0.1% (vol/vol) Tween-20 (TBST-milk) and then incubated with the following primary antibodies overnight in TBST-milk at 4 ˚C: rabbit polyclonal anti-caspase-1 (A-19) (1:2,000; Santa Cruz Biotechnology), mouse monoclonal anti-caspase-4 (4B9) (1:2,000; MBL), and mouse monoclonal anti-β-actin (8H10D10) (1:20,000; Cell Signaling Technology). Blots were then incubated with anti-rabbit IgG or anti-mouse IgG horseradish peroxidase (HRP)-conjugated secondary antibodies (1:10,000; Cell Signaling) in TBST-milk for 1–2 hours at room temperature, followed by Supersignal West Femto Max Sensitivity ECL Substrate (Thermo). Chemiluminescence was detected using a GE Healthcare AI600 imager.

Quantitative real-time PCR (qPCR)

To evaluate the effect of IFNγ priming on the expression of *CASP1*, *CASP4*, *CASP5*, *IL18*, and *IL1B* in HCT116 and C2Bbe1 cells, we used Luminaris Color HiGreen qPCR Master Mix (Thermo Scientific) and a C1000 Touch Thermal Cycler, CFX96 Real-Time System (Bio Rad) with validated oligonucleotide primer pairs as we have described previously (69). Relative gene expression levels were quantified based on quantification cycle (Cq) values and normalized to the reference gene, ribosomal phosphoprotein P0 (*RPLP0*). The expression of each gene was calculated using the $2^{-\Delta Cq}$ method.

D. melanogaster infections

P. alcalifaciens were grown overnight at 37°C for 16–18 hours with shaking (220 rpm) in LB–Miller broth. Cultures (1 mL) were centrifuged at 8,000 x *g* for 90 seconds, and the bacterial pellet was washed twice in an equal volume of sterile PBS and diluted 1,000–3,000-fold in sterile PBS. Two-to-7-day old *Wolbachia*-free adult male w^{1118} flies (Bloomington Drosophila Stock Center #5905) were anesthetized with CO_2 and injected with 23 nL of diluted culture (~10–30 CFU/fly) or PBS vehicle control. Flies were maintained on standard cornmeal food at 25°C and 65% relative humidity, and surviving flies

were counted every 2–6 h p.i. In each experiment, ~50 flies were injected for each condition, and survival studies were repeated at least twice for each infectious dose (~10 and ~30 CFU/fly).

Bovine ligated jejuno-ileal loop infections

Jersey, Holstein, or cross-bred calves were obtained from North Carolina State University or University of Wisconsin farm herds. Calves were separated from the dam and transferred to AAALAC-approved large animal housing facilities by 1 day of age. Calves were administered either colostrum or colostrum replacer, and adequate passive transfer was estimated by measurement of serum total protein. Calves were treated for 3 days with ceftiofur (4–6 mg/kg SC q24h) and/or flunixin meglumine (50 mg/kg IV q24h) if needed based on the clinical condition upon arrival. Calves were fed milk replacer at 10%–20% body weight per day with *ad libitum* access to water and hay.

At 3 to 6 weeks of age, calves were anesthetized with intravenous propofol and maintained on isoflurane inhalant for ligated jejuno-ileal loop surgery as previously described (125). Briefly, calves were placed in left lateral recumbency, and a right flank incision was made. Sixteen to thirty-eight 4- to 6-cm loops were tied within the ileum and terminal jejunum, leaving 1-cm spacers between adjacent loops. Prior to inoculation, loop lengths were recorded. Loops injected with vehicle only served as negative controls. Loops were infected individually with 3 mL LB (12-h incubation) or 2 mL PBS (2-h and 8-h incubation) containing approximately 10^9 CFU of *P. alcalifaciens*. The intestine was returned to the abdomen, the incision was closed, and the calves were monitored under inhalant anesthesia for the duration of the experiment. At 2 h, 8 h, or 12 h p.i., the incision was opened, and each loop was individually excised. Calves were euthanized by intravenous pentobarbital.

In preparation for ligated loop infections, bacteria were grown shaking (225 rpm) overnight at 37°C in LB–Miller broth. For the 12 h infections, overnight cultures were subcultured 1:100 into LB–Miller broth and further incubated for 3.5–4 hours at 37°C with shaking (225 rpm). Bacteria were washed twice and resuspended in PBS (2 hours or 8 hours) or LB (12 hours) with bacterial normalization based on optical density (OD_{600}) for a final inoculation dose of ~10^9 *P. alcalifaciens* per loop. The actual inoculum dose was determined by serial dilution and plating. Following loop excision, intestinal fluid and tissue samples were harvested and processed separately. The fluid volume was calculated by excising individual loops and weighing escaped luminal fluid on a sterile Petri dish. Luminal fluid was then transferred to 1 mL sterile PBS to allow for bacterial enumeration. Intestinal tissue was washed twice in sterile PBS to remove non-adherent bacteria and ingesta and then added to 5 mL sterile PBS. For 2 h and 8 h infections, washed tissues were cut in half with one segment treated with gentamicin (50 µg/mL) for 30 minutes at 37 ˚C to quantify intracellular bacteria, and the remaining half was processed to quantify tissue-associated bacteria. After gentamicin treatment, tissues were washed twice with PBS to remove remaining antibiotics. Samples were subsequently homogenized, serially diluted in PBS, and plated for CFU enumeration.

The Institutional Animal Care and Use Committees of North Carolina State University and University of Wisconsin-Madison approved all animal experiments (NCSU protocol numbers 15–047-B and 17–186-B; UW-Madison protocol number V006249). All animal experiments were performed in accordance with the PHS "Guide for the Care and Use of Laboratory Animals" in AAALAC-approved animal facilities.

Histopathology

Intestinal samples were fixed in 10% neutral buffered formalin, processed for paraffin embedding, sectioned (5 µm), and stained with hematoxylin and eosin for histologic analyses. Tissues were assessed and scored by an American College of Veterinary Pathology (ACVP) board-certified pathologist with a scoring system derived from previously published rubrics (126, 127). The following criteria were scored from 0 to

TABLE 1 Histopathology scoring system

Score	Lamina propria neutrophil accumulation	Submucosal edema	Epithelial damage	Crypt abscess	Villus blunting	Cell death
0	0–5/hpf	No change (0–5)	No change	None	Normal villi	Absence of cells with morphological features of death
1	6–20/hpf	5–10	Detectable (<10%)	Detectable (<10%)	Few villi mildly blunted	Few sporadic necrotic/apoptotic cells detected
2	21–60/hpf	11–20	Mild (10%–20%)	Mild (10%–20%)	Most villi mildly blunted	Minimal number of necrotic/apoptotic cells detected
3	61–100/hpf	21–40	Moderate (21%–40%)	Moderate (21%–40%)	Most villi moderately blunted	Moderate number of necrotic/apoptotic cells detected
4	>100/hpf	>40	Marked (>40%)	Marked (>40%)	All villi severely blunted	Large number of necrotic/apoptotic cells detected

4: lamina propria neutrophil accumulation, submucosal edema, epithelial damage, crypt abscess, villus blunting, and cell death (Table 1).

Statistical analysis

Statistical analysis was performed using GraphPad Prism 10 software. Statistical significance of comparisons between treatment groups was determined using either an unpaired, two-tailed Student's *t* test, or for group analysis, using one-way analysis of variance (ANOVA) followed by Dunnett's multiple-comparison test. For survival curves in flies, a logrank test (Mantel–Cox method) was used to compare two groups.

ACKNOWLEDGMENTS

We thank Drs. Allis Chien and Ryan Leib at Stanford University Mass Spectrometry (SUMS) facility for mass spectrometry analysis, the staff at the Franceschi Microscopy and Imaging Center (FMIC) at Washington State University for their expertise and use of electron microscope facilities, Patricia Reis for her technical assistance in the initial stages of this project, Dr. J. Michael Janda for his help in sourcing the *P. alcalifaciens* 205/92 strain, Dr. M. John Albert for providing anti-*P. alcalifaciens* antibodies, Dr. Jason Smith for providing C2Bbe1 cells, Dr. Harry Mobley and Stephanie Himpsl for providing pGEN-DsRed.T3 and pGEN-MCS plasmids, Dr. Petra Dersch for providing the pFU35 plasmid, and Dr. David Rasko for his comments on the manuscript.

Research reported in this publication was supported, in part, by a Burroughs Wellcome Fund Investigators in the Pathogenesis of Infectious Diseases Award to L.A.K., and the National Institute of Allergy and Infectious Diseases (NIAID) of the National Institutes of Health (NIH) under award numbers R21AI130645 to L.A.K. and R01AI134766 to L.A.K and B.A.V. The funders had no role in study design, data collection and interpretation, or the decision to submit the work for publication. J.A.K. is currently employed by Genentech Inc. Genentech Inc. was not involved in this study or its design.

AUTHOR AFFILIATIONS

[1]Paul G. Allen School for Global Health, College of Veterinary Medicine, Washington State University, Pullman, Washington, USA
[2]Wellcome Sanger Institute, Hinxton, Cambridgeshire, United Kingdom
[3]Department of Pathobiological Sciences, School of Veterinary Medicine, University of Wisconsin-Madison, Madison, Wisconsin, USA

[4]Department of Clinical Sciences, College of Veterinary Medicine, North Carolina State University, Raleigh, North Carolina, USA
[5]Public Health Laboratory, Los Angeles County Department of Public Health, Downey, California, USA
[6]Division of Gastroenterology, Hepatology and Nutrition, BC Children's Hospital and the University of British Columbia, Vancouver, British Columbia, Canada
[7]Department of Microbiology and Molecular Genetics, University of California, Irvine, California, USA
[8]Comparative Pathology Laboratory, Research Animal Resources and Compliance, University of Wisconsin-Madison, Madison, Wisconsin, USA
[9]School of Molecular Biosciences, College of Veterinary Medicine, Washington State University, Pullman, Washington, USA
[10]Department of Microbiology and Molecular Genetics, Robert Larner College of Medicine at The University of Vermont, Burlington, Vermont, USA

PRESENT ADDRESS

Jessica A. Klein, Complex in vitro Systems, Safety Assessment, Genentech Inc., South San Francisco, California, USA
Marie Wrande, Department of Medical Biochemistry and Microbiology, Uppsala University, Uppsala, Sweden

AUTHOR ORCIDs

Jessica A. Klein http://orcid.org/0000-0002-0529-9406
Alexander V. Predeus http://orcid.org/0000-0002-2750-1599
Nicole M. Green http://orcid.org/0000-0001-9745-0240
Michael McClelland http://orcid.org/0000-0003-1788-9347
Alan G. Goodman http://orcid.org/0000-0001-6394-332X
Johanna R. Elfenbein http://orcid.org/0000-0002-4764-0713
Leigh A. Knodler http://orcid.org/0000-0002-3028-2198

AUTHOR CONTRIBUTIONS

Jessica A. Klein, Conceptualization, Data curation, Formal analysis, Investigation, Methodology, Visualization, Writing – original draft | Alexander V. Predeus, Data curation, Formal analysis, Methodology, Visualization, Writing – original draft | Aimee R. Greissl, Formal analysis, Investigation, Methodology, Writing – review and editing | Mattie M. Clark-Herrera, Formal analysis, Investigation, Methodology, Writing – review and editing | Eddy Cruz, Formal analysis, Investigation, Methodology, Writing – review and editing | Jennifer A. Cundiff, Formal analysis, Investigation, Writing – review and editing | Amanda L. Haeberle, Formal analysis, Investigation, Methodology, Writing – review and editing | Maya Howell, Investigation, Writing – review and editing | Aaditi Lele, Formal analysis, Investigation, Methodology, Writing – review and editing | Donna J. Robinson, Investigation, Methodology, Writing – review and editing | Trina L. Westerman, Investigation, Methodology, Writing – review and editing | Marie Wrande, Investigation, Methodology, Writing – review and editing | Sarah J. Wright, Investigation, Methodology, Writing – review and editing | Nicole M. Green, Resources, Writing – review and editing | Bruce A. Vallance, Conceptualization, Funding acquisition, Writing – review and editing | Michael McClelland, Formal analysis, Investigation, Writing – review and editing | Andres Mejia, Formal analysis, Investigation, Methodology, Writing – review and editing | Alan G. Goodman, Formal analysis, Investigation, Methodology, Writing – review and editing | Johanna R. Elfenbein, Formal analysis, Investigation, Methodology, Writing – review and editing | Leigh A. Knodler, Conceptualization, Data curation, Formal analysis, Funding acquisition, Investigation, Methodology, Project administration, Supervision, Visualization, Writing – original draft

DIRECT CONTRIBUTION

This article is a direct contribution from Leigh Knodler, a member of the *Infection and Immunity* Editorial Board, who arranged for and secured reviews by Cammie Lesser, Massachusetts General Hospital, and Kimberly Walker, University of North Carolina at Chapel Hill.

ADDITIONAL FILES

The following material is available online.

Supplemental Material

Supplemental figures (IAI00314-24-s0001.pdf). Fig. S1-S4.
Table S1 (IAI00314-24-s0002.xlsx). *P. alcalifaciens* genome information used for analysis.
Table S2 (IAI00314-24-s0003.docx). Oligos used for cloning.

REFERENCES

1. Ferraresso J, Lawton B, Bayliss S, Sheppard S, Cardazzo B, Gaze W, Buckling A, Vos M. 2020. Determining the prevalence, identity and possible origin of bacterial pathogens in soil. Environ Microbiol 22:5327–5340. https://doi.org/10.1111/1462-2920.15243
2. Gessew GT, Desta AF, Adamu E. 2022. High burden of multidrug resistant bacteria detected in Little Akaki River. Comp Immunol Microbiol Infect Dis 80:101723. https://doi.org/10.1016/j.cimid.2021.101723
3. Paiva MC, Reis MP, Costa PS, Dias MF, Bleicher L, Scholte LLS, Nardi RMD, Nascimento AMA. 2017. Identification of new bacteria harboring *qnrS* and *aac(6')-Ib/cr* and mutations possibly involved in fluoroquinolone resistance in raw sewage and activated sludge samples from a full-scale WWTP. Water Res 110:27–37. https://doi.org/10.1016/j.watres.2016.11.056
4. Shima A, Hinenoya A, Samosornsuk W, Samosornsuk S, Mungkornkaew N, Yamasaki S. 2016. Prevalence of *Providencia* strains among patients with diarrhea and in retail meats in Thailand. Jpn J Infect Dis 69:323–325. https://doi.org/10.7883/yoken.JJID.2015.224
5. Dl H, Liang S, Li Q, Shi L, Shima A, Meng H, Yan H, Yamasaki S. 2018. *Providencia* in retail meats from Guangzhou, China and Osaka, Japan: prevalence, antimicrobial resistance and characterization of classes 1, 2 and 3 integrons. J Vet Med Sci 80:829–835. https://doi.org/10.1292/jvms.18-0037
6. Viswanathan P, Kaur R. 2001. Prevalence and growth of pathogens on salad vegetables, fruits and sprouts. Int J Hyg Environ Health 203:205–213. https://doi.org/10.1078/S1438-4639(04)70030-9
7. Abdelnoor AM, Batshoun R, Roumani BM. 1983. The bacterial flora of fruits and vegetables in Lebanon and the effect of washing on the bacterial content. Zentralbl Bakteriol Mikrobiol Hyg B 177:342–349.
8. Burns MB, Lynch J, Starr TK, Knights D, Blekhman R. 2015. Virulence genes are a signature of the microbiome in the colorectal tumor microenvironment. Genome Med 7:55. https://doi.org/10.1186/s13073-015-0177-8
9. Lim MY, Yoon HS, Rho M, Sung J, Song Y-M, Lee K, Ko G. 2016. Analysis of the association between host genetics, smoking, and sputum microbiota in healthy humans. Sci Rep 6:23745. https://doi.org/10.1038/srep23745
10. Baker JL, Hendrickson EL, Tang X, Lux R, He X, Edlund A, McLean JS, Shi W. 2019. *Klebsiella* and *Providencia* emerge as lone survivors following long-term starvation of oral microbiota. Proc Natl Acad Sci U S A 116:8499–8504. https://doi.org/10.1073/pnas.1820594116
11. Zambruni M, Ochoa TJ, Somasunderam A, Cabada MM, Morales ML, Mitreva M, Rosa BA, Acosta GJ, Vigo NI, Riveros M, Arango S, Durand D, Berends MN, Melby P, Utay NS. 2019. Stunting is preceded by intestinal mucosal damage and microbiome changes and is associated with systemic inflammation in a cohort of Peruvian infants. Am J Trop Med Hyg 101:1009–1017. https://doi.org/10.4269/ajtmh.18-0975
12. Leite GGS, Morales W, Weitsman S, Celly S, Parodi G, Mathur R, Sedighi R, Barlow GM, Rezaie A, Pimentel M. 2019. Optimizing microbiome sequencing for small intestinal aspirates: validation of novel techniques through the REIMAGINE study. BMC Microbiol 19:239. https://doi.org/10.1186/s12866-019-1617-1
13. Galac MR, Lazzaro BP. 2011. Comparative pathology of bacteria in the genus *Providencia* to a natural host, *Drosophila melanogaster*. Microbes Infect 13:673–683. https://doi.org/10.1016/j.micinf.2011.02.005
14. Jackson TJ, Wang H, Nugent MJ, Griffin CT, Burnell AM, Dowds BCA. 1995. Isolation of insect pathogenic bacteria, *Providencia rettgeri*, from *Heterorhabditis* spp. J Appl Bacteriol 78:237–244. https://doi.org/10.1111/j.1365-2672.1995.tb05022.x
15. Corby-Harris V, Pontaroli AC, Shimkets LJ, Bennetzen JL, Habel KE, Promislow DEL. 2007. Geographical distribution and diversity of bacteria associated with natural populations of *Drosophila melanogaster*. Appl Environ Microbiol 73:3470–3479. https://doi.org/10.1128/AEM.02120-06
16. Juneja P. 2011. Short term evolution in the immune response of *Drosophila melanogaster*: insights from studies of population genetics and the epidemiology of bacterial infection, Cornell University
17. Ksentini I, Gharsallah H, Sahnoun M, Schuster C, Hamli Amri S, Gargouri R, Triki MA, Ksantini M, Leclerque A. 2019. *Providencia entomophila* sp. nov., a new bacterial species associated with major olive pests in Tunisia. PLoS One 14:e0223943. https://doi.org/10.1371/journal.pone.0223943
18. Kuzina LV, Peloquin JJ, Vacek DC, Miller TA. 2001. Isolation and identification of bacteria associated with adult laboratory Mexican fruit flies, *Anastrepha ludens* (Diptera: Tephritidae). Curr Microbiol 42:290–294. https://doi.org/10.1007/s002840110219
19. Salas B, Conway HE, Vacek DC, Vitek C, Schuenzel EL. 2023. Pathogenicity of multiple *Providencia* species (Enterobacteriales: Morganellaceae) to the mass-reared Mexican fruit fly (Diptera: Tephritidae). J Insect Sci 23:4. https://doi.org/10.1093/jisesa/iead024
20. O'Hara CM, Brenner FW, Miller JM. 2000. Classification, identification, and clinical significance of *Proteus*, *Providencia*, and *Morganella*. Clin Microbiol Rev 13:534–546. https://doi.org/10.1128/CMR.13.4.534
21. Yoh M, Matsuyama J, Ohnishi M, Takagi K, Miyagi H, Mori K, Park K-S, Ono T, Honda T. 2005. Importance of *Providencia* species as a major cause of travellers' diarrhoea. J Med Microbiol 54:1077–1082. https://doi.org/10.1099/jmm.0.45846-0
22. Stock I, Wiedemann B. 1998. Natural antibiotic susceptibility of *Providencia stuartii*, *P. rettgeri*, *P. alcalifaciens* and *P. rustigianii* strains. J Med Microbiol 47:629–642. https://doi.org/10.1099/00222615-47-7-629
23. Guan J, Bao C, Wang P, Jing Y, Wang L, Li X, Mu X, Li B, Zhou D, Guo X, Yin Z. 2022. Genetic characterization of four groups of chromosome-borne accessory genetic elements carrying drug resistance genes in *Providencia*. Infect Drug Resist 15:2253–2270. https://doi.org/10.2147/IDR.S354934
24. Wang P, Li C, Yin Z, Jiang X, Li X, Mu X, Wu N, Chen F, Zhou D. 2023. Genomic epidemiology and heterogeneity of *Providencia* and their

blaNDM-1-carrying plasmids. Emerg Microbes Infect 12:2275596. https://doi.org/10.1080/22221751.2023.2275596
25. Boattini M, Bianco G, Llorente LI, Acero LA, Nunes D, Seruca M, Mendes VS, Almeida A, Bastos P, Rodríguez-Villodres Á, et al. 2024. *Enterobacterales* carrying chromosomal AmpC β-lactamases in Europe (EuESCPM): epidemiology and antimicrobial resistance burden from a cohort of 27 hospitals, 2020-2022. Int J Antimicrob Agents 63:107115. https://doi.org/10.1016/j.ijantimicag.2024.107115
26. Ridge LE, Thomas ME. 1955. Infection with the Providence type of paracolon bacillus in a residential nursery. J Pathol Bacteriol 69:334–337.
27. Prakash OM, Dayal S, Kalra SL, Prakash OM, Dayal S, Kalra SL. 1966. Bacterial aetiology of infantile diarrhoea in a village population with observations on some Providence strains isolated from diarrhoea and non-diarrhoea cases. Indian J Med Res 54:705–713.
28. Bhat P, Myers RM, Feldman RA. 1971. Providence group of organisms in the aetiology of juvenile diarrhoea. Indian J Med Res 59:1010–1018.
29. Albert MJ, Faruque ASG, Mahalanabis D. 1998. Association of *Providencia alcalifaciens* with diarrhea in children. J Clin Microbiol 36:1433–1435. https://doi.org/10.1128/JCM.36.5.1433-1435.1998
30. M. Al-Rawi A, A. Yonan M. 2009. Isolation and identification of *Providencia alcalifaciens* from infantile diarrhea and study of the histological changes that it cause. Rafidain J Sci 20:37–48. https://doi.org/10.33899/rjs.2009.40182
31. Murata T, Iida T, Shiomi Y, Tagomori K, Akeda Y, Yanagihara I, Mushiake S, Ishiguro F, Honda T. 2001. A large outbreak of foodborne infection attributed to *Providencia alcalifaciens*. J Infect Dis 184:1050–1055. https://doi.org/10.1086/323458
32. Chlibek R, Jirous J, Beran J. 2002. Diarrhea outbreak among Czech army field hospital personnel caused by *Providencia alcalifaciens*. J Travel Med 9:151–152. https://doi.org/10.2310/7060.2002.23190
33. Shah MM, Odoyo E, Larson PS, Apondi E, Kathiiko C, Miringu G, Nakashima M, Ichinose Y. 2015. Report of a foodborne *Providencia alcalifaciens* outbreak in Kenya. Am J Trop Med Hyg 93:497–500. https://doi.org/10.4269/ajtmh.15-0126
34. Shah M, Kathiiko C, Wada A, Odoyo E, Bundi M, Miringu G, Guyo S, Karama M, Ichinose Y. 2016. Prevalence, seasonal variation, and antibiotic resistance pattern of enteric bacterial pathogens among hospitalized diarrheic children in suburban regions of central Kenya. Trop Med Health 44:39. https://doi.org/10.1186/s41182-016-0038-1
35. Haynes J, Hawkey PM. 1989. *Providencia alcalifaciens* and travellers' diarrhoea. BMJ 299:94–95. https://doi.org/10.1136/bmj.299.6691.94-a
36. Möhr AJ, van der Lugt JJ, Josling D, Picard J, van der Merwe LL. 2002. Primary bacterial enteritis caused by *Providencia alcalifaciens* in three dogs. Vet Rec 150:52–53. https://doi.org/10.1136/vr.150.2.52
37. Tribe GW, Rood MJ. 2002. *Providencia alcalifaciens* in diarrhoeic dogs and cats. Vet Rec 150:386–387.
38. Król J, Janeczek M, Pliszczak-Król A, Janeczek W, Florek M. 2007. *Providencia alcalifaciens* as the presumptive cause of diarrhoea in dog. Pol J Vet Sci 10:285–287.
39. Jørgensen HJ, Valheim M, Sekse C, Bergsjø BA, Wisløff H, Nørstebø SF, Skancke E, Lagesen K, Haaland AH, Rodriguez-Campos S, Sjurseth SK, Hofshagen M, Jarp J, Tronerud O-H, Johannessen GS, Heggelund M, Rygg S, Christensen E, Boye M, Gjerset B, Sandvik M, Soltvedt EM, Wolff C. 2021. An official outbreak investigation of acute haemorrhagic diarrhoea in dogs in Norway points to *Providencia alcalifaciens* as a likely cause. Animals (Basel) 11:3201. https://doi.org/10.3390/ani11113201
40. Albert MJ, Alam K, Ansaruzzaman M, Islam MM, Rahman AS, Haider K, Bhuiyan NA, Nahar S, Ryan N, Montanaro J. 1992. Pathogenesis of *Providencia alcalifaciens*-induced diarrhea. Infect Immun 60:5017–5024. https://doi.org/10.1128/iai.60.12.5017-5024.1992
41. Mathan MM, Mathan VI, Albert MJ. 1993. Electron microscopic study of the attachment and penetration of rabbit intestinal epithelium by *Providencia alcalifaciens*. J Pathol 171:67–71. https://doi.org/10.1002/path.1711710114
42. Shima A, Hinenoya A, Asakura M, Sugimoto N, Tsukamoto T, Ito H, Nagita A, Faruque SM, Yamasaki S. 2012. Molecular characterizations of cytolethal distending toxin produced by *Providencia alcalifaciens* strains isolated from patients with diarrhea. Infect Immun 80:1323–1332. https://doi.org/10.1128/IAI.05831-11
43. Albert MJ, Ansaruzzaman M, Bhuiyan NA, Neogi PK, Faruque AS. 1995. Characteristics of invasion of HEp-2 cells by *Providencia alcalifaciens*. J Med Microbiol 42:186–190. https://doi.org/10.1099/00222615-42-3-186
44. Guth BEC, Perrella E. 1996. Prevalence of invasive ability and other virulence-associated characteristics in *Providencia alcalifaciens* strains isolated in São Paulo, Brazil. J Med Microbiol 45:459–462. https://doi.org/10.1099/00222615-45-6-459
45. Magalhães V, Leal NC, Melo VM, Sobreira M, Magalhães M. 1996. Invasion of HeLa cells by *Providencia alcalifaciens* presumably is plasmid-encoded. Mem Inst Oswaldo Cruz 91:767–768. https://doi.org/10.1590/s0074-02761996000600022
46. Janda JM, Abbott SL, Woodward D, Khashe S. 1998. Invasion of HEp-2 and other eukaryotic cell lines by Providenciae: further evidence supporting the role of *Providencia alcalifaciens* in bacterial gastroenteritis. Curr Microbiol 37:159–165. https://doi.org/10.1007/s002849900357
47. Sobreira M, Leal NC, Magalhães M, Guth BEC, Almeida AMP. 2001. Molecular analysis of clinical isolates of *Providencia alcalifaciens*. J Med Microbiol 50:29–34. https://doi.org/10.1099/0022-1317-50-1-29
48. Vieira ABR, Koh IHJ, Guth BEC. 2003. *Providencia alcalifaciens* strains translocate from the gastrointestinal tract and are resistant to lytic activity of serum complement. J Med Microbiol 52:633–636. https://doi.org/10.1099/jmm.0.04993-0
49. Maszewska A, Torzewska A, Staczek P, Rózalski A. 2010. Enterocyte-like Caco-2 cells as a model for *in vitro* studies of diarrhoeagenic *Providencia alcalifaciens* invasion. Microb Pathog 49:285–293. https://doi.org/10.1016/j.micpath.2010.06.010
50. Yuan C, Wei Y, Zhang S, Cheng J, Cheng X, Qian C, Wang Y, Zhang Y, Yin Z, Chen H. 2020. Comparative genomic analysis reveals genetic mechanisms of the variety of pathogenicity, antibiotic resistance, and environmental adaptation of *Providencia* genus. Front Microbiol 11:572642. https://doi.org/10.3389/fmicb.2020.572642
51. Klein JA, Dave BM, Raphenya AR, McArthur AG, Knodler LA. 2017. Functional relatedness in the Inv/Mxi-Spa type III secretion system family. Mol Microbiol 103:973–991. https://doi.org/10.1111/mmi.13602
52. Dale C, Jones T, Pontes M. 2005. Degenerative evolution and functional diversification of type-III secretion systems in the insect endosymbiont *Sodalis glossinidius*. Mol Biol Evol 22:758–766. https://doi.org/10.1093/molbev/msi061
53. Foultier B, Troisfontaines P, Müller S, Opperdoes FR, Cornelis GR. 2002. Characterization of the ysa pathogenicity locus in the chromosome of *Yersinia enterocolitica* and phylogeny analysis of type III secretion systems. J Mol Evol 55:37–51. https://doi.org/10.1007/s00239-001-0089-7
54. Peterson J, Garges S, Giovanni M, McInnes P, Wang L, Schloss JA, Bonazzi V, McEwen JE, Wetterstrand KA, Deal C, et al. 2009. The NIH human microbiome project. Genome Res 19:2317–2323. https://doi.org/10.1101/gr.096651.109
55. Dong X, Jia H, Yu Y, Xiang Y, Zhang Y. 2024. Genomic revisitation and reclassification of the genus *Providencia*. mSphere 9:e0073123. https://doi.org/10.1128/msphere.00731-23
56. Kaniga K, Trollinger D, Galán JE. 1995. Identification of two targets of the type III protein secretion system encoded by the *inv* and *spa* loci of *Salmonella typhimurium* that have homology to the *Shigella* IpaD and IpaA proteins. J Bacteriol 177:7078–7085. https://doi.org/10.1128/jb.177.24.7078-7085.1995
57. Kubori T, Sukhan A, Aizawa S-I, Galán JE. 2000. Molecular characterization and assembly of the needle complex of the *Salmonella typhimurium* type III protein secretion system. Proc Natl Acad Sci U S A 97:10225–10230. https://doi.org/10.1073/pnas.170128997
58. Lilic M, Galkin VE, Orlova A, VanLoock MS, Egelman EH, Stebbins CE. 2003. *Salmonella* SipA polymerizes actin by stapling filaments with nonglobular protein arms. Science 301:1918–1921. https://doi.org/10.1126/science.1088433
59. Collazo CM, Galán JE. 1997. The invasion-associated type III system of *Salmonella typhimurium* directs the translocation of Sip proteins into the host cell. Mol Microbiol 24:747–756. https://doi.org/10.1046/j.1365-2958.1997.3781740.x
60. Ibarra JA, Knodler LA, Sturdevant DE, Virtaneva K, Carmody AB, Fischer ER, Porcella SF, Steele-Mortimer O. 2010. Induction of *Salmonella* pathogenicity island 1 under different growth conditions can affect

Salmonella-host cell interactions *in vitro*. Microbiol (Reading) 156:1120–1133. https://doi.org/10.1099/mic.0.032896-0
61. Romero S, Grompone G, Carayol N, Mounier J, Guadagnini S, Prevost M-C, Sansonetti PJ, Van Nhieu GT. 2011. ATP-mediated Erk1/2 activation stimulates bacterial capture by filopodia, which precedes *Shigella* invasion of epithelial cells. Cell Host Microbe 9:508–519. https://doi.org/10.1016/j.chom.2011.05.005
62. Uliczka F, Pisano F, Schaake J, Stolz T, Rohde M, Fruth A, Strauch E, Skurnik M, Batzilla J, Rakin A, Heesemann J, Dersch P. 2011. Unique cell adhesion and invasion properties of *Yersinia enterocolitica* O:3, the most frequent cause of human yersiniosis. PLoS Pathog 7:e1002117. https://doi.org/10.1371/journal.ppat.1002117
63. Kwok T, Backert S, Schwarz H, Berger J, Meyer TF. 2002. Specific entry of *Helicobacter pylori* into cultured gastric epithelial cells via a zipper-like mechanism. Infect Immun 70:2108–2120. https://doi.org/10.1128/IAI.70.4.2108-2120.2002
64. Adam T, Arpin M, Prévost MC, Gounon P, Sansonetti PJ. 1995. Cytoskeletal rearrangements and the functional role of T-plastin during entry of *Shigella flexneri* into HeLa cells. J Cell Biol 129:367–381. https://doi.org/10.1083/jcb.129.2.367
65. Walker KA, Maltez VI, Hall JD, Vitko NP, Miller VL. 2013. A phenotype at last: essential role for the *Yersinia enterocolitica* Ysa type III secretion system in a *Drosophila melanogaster* S2 cell model. Infect Immun 81:2478–2487. https://doi.org/10.1128/IAI.01454-12
66. Du J, Reeves AZ, Klein JA, Twedt DJ, Knodler LA, Lesser CF. 2016. The type III secretion system apparatus determines the intracellular niche of bacterial pathogens. Proc Natl Acad Sci U S A 113:4794–4799. https://doi.org/10.1073/pnas.1520699113
67. Knodler LA, Nair V, Steele-Mortimer O. 2014. Quantitative assessment of cytosolic *Salmonella* in epithelial cells. PLoS One 9:e84681. https://doi.org/10.1371/journal.pone.0084681
68. Klein JA, Powers TR, Knodler LA. 2017. Measurement of *Salmonella enterica* internalization and vacuole lysis in epithelial cells. Methods Mol Biol 1519:285–296. https://doi.org/10.1007/978-1-4939-6581-6_19
69. Knodler LA, Crowley SM, Sham HP, Yang H, Wrande M, Ma C, Ernst RK, Steele-Mortimer O, Celli J, Vallance BA. 2014. Noncanonical inflammasome activation of caspase-4/caspase-11 mediates epithelial defenses against enteric bacterial pathogens. Cell Host Microbe 16:249–256. https://doi.org/10.1016/j.chom.2014.07.002
70. Sellin ME, Müller AA, Felmy B, Dolowschiak T, Diard M, Tardivel A, Maslowski KM, Hardt W-D. 2014. Epithelium-intrinsic NAIP/NLRC4 inflammasome drives infected enterocyte expulsion to restrict *Salmonella* replication in the intestinal mucosa. Cell Host Microbe 16:237–248. https://doi.org/10.1016/j.chom.2014.07.001
71. Rauch I, Deets KA, Ji DX, von Moltke J, Tenthorey JL, Lee AY, Philip NH, Ayres JS, Brodsky IE, Gronert K, Vance RE. 2017. NAIP-NLRC4 inflammasomes coordinate intestinal epithelial cell expulsion with eicosanoid and IL-18 release via activation of caspase-1 and -8. Immunity 46:649–659. https://doi.org/10.1016/j.immuni.2017.03.016
72. Song-Zhao GX, Srinivasan N, Pott J, Baban D, Frankel G, Maloy KJ. 2014. Nlrp3 activation in the intestinal epithelium protects against a mucosal pathogen. Mucosal Immunol 7:763–774. https://doi.org/10.1038/mi.2013.94
73. Crowley SM, Han X, Allaire JM, Stahl M, Rauch I, Knodler LA, Vallance BA. 2020. Intestinal restriction of *Salmonella* Typhimurium requires caspase-1 and caspase-11 epithelial intrinsic inflammasomes. PLoS Pathog 16:e1008498. https://doi.org/10.1371/journal.ppat.1008498
74. Ossina NK, Cannas A, Powers VC, Fitzpatrick PA, Knight JD, Gilbert JR, Shekhtman EM, Tomei LD, Umansky SR, Kiefer MC. 1997. Interferon-gamma modulates a p53-independent apoptotic pathway and apoptosis-related gene expression. J Biol Chem 272:16351–16357. https://doi.org/10.1074/jbc.272.26.16351
75. Jarry A, Vallette G, Cassagnau E, Moreau A, Bou-Hanna C, Lemarre P, Letessier E, Le Neel JC, Galmiche JP, Laboisse CL. 1999. Interleukin 1 and interleukin 1beta converting enzyme (caspase 1) expression in the human colonic epithelial barrier. Caspase 1 downregulation in colon cancer. Gut 45:246–251. https://doi.org/10.1136/gut.45.2.246
76. Lin XY, Choi MS, Porter AG. 2000. Expression analysis of the human caspase-1 subfamily reveals specific regulation of the CASP5 gene by lipopolysaccharide and interferon-gamma. J Biol Chem 275:39920–39926. https://doi.org/10.1074/jbc.M007255200
77. Weiss ES, Girard-Guyonvarc'h C, Holzinger D, de Jesus AA, Tariq Z, Picarsic J, Schiffrin EJ, Foell D, Grom AA, Ammann S, Ehl S, Hoshino T, Goldbach-Mansky R, Gabay C, Canna SW. 2018. Interleukin-18 diagnostically distinguishes and pathogenically promotes human and murine macrophage activation syndrome. Blood 131:1442–1455. https://doi.org/10.1182/blood-2017-12-820852
78. Naseer N, Zhang J, Bauer R, Constant DA, Nice TJ, Brodsky IE, Rauch I, Shin S. 2022. *Salmonella enterica* serovar Typhimurium induces NAIP/NLRC4- and NLRP3/ASC-independent, caspase-4-dependent inflammasome activation in human intestinal epithelial cells. Infect Immun 90:e0066321. https://doi.org/10.1128/iai.00663-21
79. Holly MK, Han X, Zhao EJ, Crowley SM, Allaire JM, Knodler LA, Vallance BA, Smith JG. 2020. *Salmonella enterica* infection of murine and human enteroid-derived monolayers elicits differential activation of epithelium-intrinsic inflammasomes. Infect Immun 88:e00017-20. https://doi.org/10.1128/IAI.00017-20
80. Westerman TL, McClelland M, Elfenbein JR. 2021. YeiE regulates motility and gut colonization in *Salmonella enterica* serotype Typhimurium. mBio 12:e0368020. https://doi.org/10.1128/mBio.03680-20
81. Shaka M, Arias-Rojas A, Hrdina A, Frahm D, Iatsenko I. 2022. Lipopolysaccharide -mediated resistance to host antimicrobial peptides and hemocyte-derived reactive-oxygen species are the major *Providencia alcalifaciens* virulence factors in *Drosophila melanogaster*. PLoS Pathog 18:e1010825. https://doi.org/10.1371/journal.ppat.1010825
82. Coombes BK. 2009. Type III secretion systems in symbiotic adaptation of pathogenic and non-pathogenic bacteria. Trends Microbiol 17:89–94. https://doi.org/10.1016/j.tim.2008.11.006
83. Abby SS, Rocha EPC. 2012. The non-flagellar type III secretion system evolved from the bacterial flagellum and diversified into host-cell adapted systems. PLoS Genet 8:e1002983. https://doi.org/10.1371/journal.pgen.1002983
84. Correa VR, Majerczak DR, Ammar E-D, Merighi M, Pratt RC, Hogenhout SA, Coplin DL, Redinbaugh MG. 2012. The bacterium *Pantoea stewartii* uses two different type III secretion systems to colonize its plant host and insect vector. Appl Environ Microbiol 78:6327–6336. https://doi.org/10.1128/AEM.00892-12
85. Galac MR, Lazzaro BP. 2012. Comparative genomics of bacteria in the genus *Providencia* isolated from wild *Drosophila melanogaster*. BMC Genomics 13:612. https://doi.org/10.1186/1471-2164-13-612
86. Andolfo G, Schuster C, Gharsa HB, Ruocco M, Leclerque A. 2021. Genomic analysis of the nomenclatural type strain of the nematode-associated entomopathogenic bacterium *Providencia vermicola*. BMC Genomics 22:708. https://doi.org/10.1186/s12864-021-08027-w
87. Golubeva YA, Sadik AY, Ellermeier JR, Slauch JM. 2012. Integrating global regulatory input into the *Salmonella* pathogenicity island 1 type III secretion system. Genetics 190:79–90. https://doi.org/10.1534/genetics.111.132779
88. Thijs IMV, De Keersmaecker SCJ, Fadda A, Engelen K, Zhao H, McClelland M, Marchal K, Vanderleyden J. 2007. Delineation of the *Salmonella enterica* serovar Typhimurium HilA regulon through genome-wide location and transcript analysis. J Bacteriol 189:4587–4596. https://doi.org/10.1128/JB.00178-07
89. Aardal AM, Soltvedt EM, Nørstebø SF, Haverkamp THA, Rodriguez-Campos S, Skancke E, Llarena A-K. 2024. Defining a metagenomic threshold for detecting low abundances of *Providencia alcalifaciens* in canine faecal samples. Front Cell Infect Microbiol 14:1305742. https://doi.org/10.3389/fcimb.2024.1305742
90. Salama AM, Helmy EA, Abd El-ghany TM, Ganash M. 2021. Nickel oxide nanoparticles application for enhancing biogas production using certain wastewater bacteria and aquatic macrophytes biomass. Waste Biomass Valor 12:2059–2070. https://doi.org/10.1007/s12649-020-01144-9
91. Bulach D, Carter GP, Albert MJ. 2024. Enteropathogenic *Providencia alcalifaciens*: a subgroup of *P. alcalifaciens* that causes diarrhea. Microorganisms 12:1479. https://doi.org/10.3390/microorganisms12071479
92. Murli S, Watson RO, Galán JE. 2001. Role of tyrosine kinases and the tyrosine phosphatase SptP in the interaction of *Salmonella* with host cells. Cell Microbiol 3:795–810. https://doi.org/10.1046/j.1462-5822.2001.00158.x

93. Fu Y, Galán JE. 1999. A *Salmonella* protein antagonizes Rac-1 and Cdc42 to mediate host-cell recovery after bacterial invasion. Nat New Biol 401:293–297. https://doi.org/10.1038/45829
94. Elliott SJ, Krejany EO, Mellies JL, Robins-Browne RM, Sasakawa C, Kaper JB. 2001. EspG, a novel type III system-secreted protein from enteropathogenic *Escherichia coli* with similarities to VirA of *Shigella flexneri*. Infect Immun 69:4027–4033. https://doi.org/10.1128/IAI.69.6.4027-4033.2001
95. Clements A, Smollett K, Lee SF, Hartland EL, Lowe M, Frankel G. 2011. EspG of enteropathogenic and enterohemorrhagic *E. coli* binds the Golgi matrix protein GM130 and disrupts the Golgi structure and function. Cell Microbiol 13:1429–1439. https://doi.org/10.1111/j.1462-5822.2011.01631.x
96. Uchiya K, Tobe T, Komatsu K, Suzuki T, Watarai M, Fukuda I, Yoshikawa M, Sasakawa C. 1995. Identification of a novel virulence gene, *virA*, on the large plasmid of *Shigella*, involved in invasion and intercellular spreading. Mol Microbiol 17:241–250. https://doi.org/10.1111/j.1365-2958.1995.mmi_17020241.x
97. Arbeloa A, Bulgin RR, MacKenzie G, Shaw RK, Pallen MJ, Crepin VF, Berger CN, Frankel G. 2008. Subversion of actin dynamics by EspM effectors of attaching and effacing bacterial pathogens. Cell Microbiol 10:1429–1441. https://doi.org/10.1111/j.1462-5822.2008.01136.x
98. Zhou D, Mooseker MS, Galán JE. 1999. Role of the *S. typhimurium* actin-binding protein SipA in bacterial internalization. Science 283:2092–2095. https://doi.org/10.1126/science.283.5410.2092
99. Van Nhieu GT. 1997. Modulation of bacterial entry into epithelial cells by association between vinculin and the *Shigella* IpaA invasin. EMBO J 16:2717–2729. https://doi.org/10.1093/emboj/16.10.2717
100. Wall DM, Nadeau WJ, Pazos MA, Shi HN, Galyov EE, McCormick BA. 2007. Identification of the *Salmonella enterica* serotype Typhimurium SipA domain responsible for inducing neutrophil recruitment across the intestinal epithelium. Cell Microbiol 9:2299–2313. https://doi.org/10.1111/j.1462-5822.2007.00960.x
101. Kodama T, Rokuda M, Park K-S, Cantarelli VV, Matsuda S, Iida T, Honda T. 2007. Identification and characterization of VopT, a novel ADP-ribosyltransferase effector protein secreted via the *Vibrio parahaemolyticus* type III secretion system 2. Cell Microbiol 9:2598–2609. https://doi.org/10.1111/j.1462-5822.2007.00980.x
102. Alam MZ, Madan R. 2024. *Clostridioides difficile* toxins: host cell interactions and their role in disease pathogenesis. Toxins (Basel) 16:241. https://doi.org/10.3390/toxins16060241
103. Dong H, Zhang X, Pan Z, Peng D, Liu X. 2008. Identification of genes for biofilm formation in a *Salmonella enteritidis* strain by transposon mutagenesis. Wei Sheng Wu Xue Bao 48:869–873.
104. Geddes K, Worley M, Niemann G, Heffron F. 2005. Identification of new secreted effectors in *Salmonella enterica* serovar Typhimurium. Infect Immun 73:6260–6271. https://doi.org/10.1128/IAI.73.10.6260-6271.2005
105. Odendall C, Rolhion N, Förster A, Poh J, Lamont DJ, Liu M, Freemont PS, Catling AD, Holden DW. 2012. The *Salmonella* kinase SteC targets the MAP kinase MEK to regulate the host actin cytoskeleton. Cell Host Microbe 12:657–668. https://doi.org/10.1016/j.chom.2012.09.011
106. Poh J, Odendall C, Spanos A, Boyle C, Liu M, Freemont P, Holden DW. 2008. SteC is a *Salmonella* kinase required for SPI-2-dependent F-actin remodelling. Cell Microbiol 10:20–30. https://doi.org/10.1111/j.1462-5822.2007.01010.x
107. Case EDR, Chong A, Wehrly TD, Hansen B, Child R, Hwang S, Virgin HW, Celli J. 2014. The *Francisella* O-antigen mediates survival in the macrophage cytosol via autophagy avoidance. Cell Microbiol 16:862–877. https://doi.org/10.1111/cmi.12246
108. Engström P, Burke TP, Tran CJ, Iavarone AT, Welch MD. 2021. Lysine methylation shields an intracellular pathogen from ubiquitylation and autophagy. Sci Adv 7:eabg2517. https://doi.org/10.1126/sciadv.abg2517
109. Tattoli I, Sorbara MT, Yang C, Tooze SA, Philpott DJ, Girardin SE. 2013. *Listeria* phospholipases subvert host autophagic defenses by stalling pre-autophagosomal structures. EMBO J 32:3066–3078. https://doi.org/10.1038/emboj.2013.234
110. Mitchell G, Ge L, Huang Q, Chen C, Kianian S, Roberts MF, Schekman R, Portnoy DA. 2015. Avoidance of autophagy mediated by PlcA or ActA is required for *Listeria monocytogenes* growth in macrophages. Infect Immun 83:2175–2184. https://doi.org/10.1128/IAI.00110-15
111. Borgo GM, Burke TP, Tran CJ, Lo NTN, Engström P, Welch MD. 2022. A patatin-like phospholipase mediates *Rickettsia parkeri* escape from host membranes. Nat Commun 13:3656. https://doi.org/10.1038/s41467-022-31351-y
112. Chander Y, Goyal SM, Gupta SC. 2006. Antimicrobial resistance of *Providencia* spp. isolated from animal manure. Vet J 172:188–191. https://doi.org/10.1016/j.tvjl.2005.01.004
113. Hawkey PM, Penner JL, Linton AH, Hawkey CA, Crisp LJ, Hinton M. 1986. Speciation, serotyping, antimicrobial sensitivity and plasmid content of Proteeae from the environment of calf-rearing units in South West England. J Hyg (Lond) 97:405–417. https://doi.org/10.1017/-s0022172400063592
114. Ayyal Al-Gburi NM. 2020. Isolation and molecular identification and antimicrobial susceptibility of *Providencia* spp. from raw cow's milk in Baghdad, Iraq. Vet Med Int 2020:8874747. https://doi.org/10.1155/2020/8874747
115. Waldhalm DG, Meinershagen WA, Frank FW. 1969. *Providencia stuartii* as an etiologic agent in neonatal diarrhea in calves. Am J Vet Res 30:1573–1575.
116. Spira WM, Sack RB, Froehlich JL. 1981. Simple adult rabbit model for *Vibrio cholerae* and enterotoxigenic *Escherichia coli* diarrhea. Infect Immun 32:739–747. https://doi.org/10.1128/iai.32.2.739-747.1981
117. Zeng T, Su H-A, Liu Y-L, Li J-F, Jiang D-X, Lu Y-Y, Qi Y-X. 2022. Serotonin modulates insect gut bacterial community homeostasis. BMC Biol 20:105. https://doi.org/10.1186/s12915-022-01319-x
118. Bulach D, Carter GP, Albert MJ. 2024. Enteropathogenic *Providencia alcalifaciens*: a subgroup of *P. alcalifaciens* that causes diarrhea. bioRxiv. https://doi.org/10.1101/2024.04.26.591277
119. Edwards RA, Keller LH, Schifferli DM. 1998. Improved allelic exchange vectors and their use to analyze 987P fimbria gene expression. Gene 207:149–157. https://doi.org/10.1016/S0378-1119(97)00619-7
120. Lane MC, Alteri CJ, Smith SN, Mobley HLT. 2007. Expression of flagella is coincident with uropathogenic *Escherichia coli* ascension to the upper urinary tract. Proc Natl Acad Sci U S A 104:16669–16674. https://doi.org/10.1073/pnas.0607898104
121. Alteri CJ, Himpsl SD, Pickens SR, Lindner JR, Zora JS, Miller JE, Arno PD, Straight SW, Mobley HLT. 2013. Multicellular bacteria deploy the type VI secretion system to preemptively strike neighboring cells. PLoS Pathog 9:e1003608. https://doi.org/10.1371/journal.ppat.1003608
122. Uliczka F, Pisano F, Kochut A, Opitz W, Herbst K, Stolz T, Dersch P. 2011. Monitoring of gene expression in bacteria during infections using an adaptable set of bioluminescent, fluorescent and colorigenic fusion vectors. PLoS One 6:e20425. https://doi.org/10.1371/journal.pone.0020425
123. Hoiseth SK, Stocker BA. 1981. Aromatic-dependent *Salmonella typhimurium* are non-virulent and effective as live vaccines. Nature New Biol 291:238–239. https://doi.org/10.1038/291238a0
124. Wick RR, Holt KE. 2022. Polypolish: short-read polishing of long-read bacterial genome assemblies. PLOS Comput Biol 18:e1009802. https://doi.org/10.1371/journal.pcbi.1009802
125. Elfenbein JR, Endicott-Yazdani T, Porwollik S, Bogomolnaya LM, Cheng P, Guo J, Zheng Y, Yang H-J, Talamantes M, Shields C, Maple A, Ragoza Y, DeAtley K, Tatsch T, Cui P, Andrews KD, McClelland M, Lawhon SD, Andrews-Polymenis H. 2013. Novel determinants of intestinal colonization of *Salmonella enterica* serotype Typhimurium identified in bovine enteric infection. Infect Immun 81:4311–4320. https://doi.org/10.1128/IAI.00874-13
126. Thiennimitr P, Winter SE, Winter MG, Xavier MN, Tolstikov V, Huseby DL, Sterzenbach T, Tsolis RM, Roth JR, Bäumler AJ. 2011. Intestinal inflammation allows *Salmonella* to use ethanolamine to compete with the microbiota. Proc Natl Acad Sci U S A 108:17480–17485. https://doi.org/10.1073/pnas.1107857108
127. Raffatellu M, Santos RL, Chessa D, Wilson RP, Winter SE, Rossetti CA, Lawhon SD, Chu H, Lau T, Bevins CL, Adams LG, Bäumler AJ. 2007. The capsule encoding the *viaB* locus reduces interleukin-17 expression and mucosal innate responses in the bovine intestinal mucosa during infection with *Salmonella enterica* serotype Typhi. Infect Immun 75:4342–4350. https://doi.org/10.1128/IAI.01571-06